Differential Regulation of the Kar3p Kinesin-related Protein by Two Associated Proteins, Cik1p and Vik1p

Brendan D. Manning, Jennifer G. Barrett, Julie A. Wallace, Howard Granok, and Michael Snyder

Department of Molecular, Cellular, and Developmental Biology, Yale University, New Haven, Connecticut 06520-8103

Abstract. The mechanisms by which kinesin-related proteins interact with other proteins to carry out specific cellular processes is poorly understood. The kinesin-related protein, Kar3p, has been implicated in many microtubule functions in yeast. Some of these functions require interaction with the Cik1 protein (Page, B.D., L.L. Satterwhite, M.D. Rose, and M. Snyder. 1994. *J. Cell Biol.* 124:507–519). We have identified a *Saccharomyces cerevisiae* gene, named *VIK1*, encoding a protein with sequence and structural similarity to Cik1p. The Vik1 protein is detected in vegetatively growing cells but not in mating pheromone-treated cells. Vik1p physically associates with Kar3p in a complex separate from that of the Kar3p-Cik1p complex. Vik1p localizes to the spindle-pole body region in a Kar3p-dependent manner. Reciprocally, concentration of Kar3p at the spindle poles during vegetative growth requires the presence of Vik1p, but not Cik1p. Phenotypic analysis suggests that Cik1p and Vik1p are involved in different Kar3p functions. Disruption of *VIK1* causes increased resistance to the microtubule depolymerizing drug benomyl and partially suppresses growth defects of *cik1Δ* mutants. The *vik1Δ* and *kar3Δ* mutations, but not *cik1Δ*, partially suppresses the temperature-sensitive growth defect of strains lacking the function of two other yeast kinesin-related proteins, Cin8p and Kip1p. Our results indicate that Kar3p forms functionally distinct complexes with Cik1p and Vik1p to participate in different microtubule-mediated events within the same cell.

Key words: kinesin • microtubules • molecular motors • cytoskeleton • *Saccharomyces cerevisiae*

MICROTUBULES are a component of all eukaryotic cytoskeletons and are essential for many diverse cellular and intracellular movements, such as flagellar motility, organelle positioning, vesicle trafficking, mitotic spindle orientation, and chromosome segregation. Two families of chemomechanical motor proteins, dynein and kinesin-related proteins, are crucial for these microtubule functions (Vale et al., 1985; Schnapp and Reese, 1989; Steuer et al., 1990; reviewed by Vale and Fletterick, 1997; Hirokawa, 1998). These proteins possess highly conserved motor domains responsible for movement along microtubules (Yang et al., 1990). The nonmotor portion of these proteins links the motor domain to a vast array of cargoes or localizes the motor to various subcellular sites (Yang et al., 1989; Afshar et al., 1995; Wittmann et al., 1998).

The family of proteins sharing a region of homology with the motor domain of conventional kinesin-heavy chain (KHC)[1] has grown enormously in recent years (reviewed by Hirokawa, 1996; Moore and Endow, 1996). These kinesin-related proteins (KRPs) have been identified in all eukaryotes from yeast to humans. KRPs vary in directionality and the position of their motor domains. Most KRPs, as well as conventional kinesin, have NH_2-terminal motor domains and travel toward the more dynamic plus ends of microtubules. Others have internally located motor domains and may also have plus-end polarity. Another subfamily of KRPs have COOH-terminal motors and travel toward the less dynamic minus ends of microtubules, the end generally associated with microtubule-organizing centers. Whereas KRPs share a high degree of sequence similarity within their motor domains, the remainder of their primary sequences are highly divergent. These variable regions are thought to interact with different proteins to mediate the functional specificity of the motor (Page et al., 1994). Recent studies have unveiled many details about the molecular structure and function of kinesin-like motor domains (Hirose et al., 1995, 1996; Arnal et al., 1996; Kull et al., 1996; Sablin et al., 1996; Gulick et al., 1998), but far

Address correspondence to Michael Snyder, Department of Molecular, Cellular, and Developmental Biology, PO Box 208103, Yale University, New Haven, CT 06520-8103. Tel.: (203) 432-6139. Fax: (203)432-6161. E-mail: michael.snyder@yale.edu

1. *Abbreviations used in this paper:* HA, hemagglutinin; HAT, HA/transposon tag; KAP, kinesin-associated protein; KHC, kinesin-heavy chain; KLC, kinesin light chain; KRP, kinesin-related protein; ORF, open reading frame; SPB, spindle-pole bodies.

less is known about how these proteins are regulated and what other components are involved in their function.

Aside from the light chains of conventional KHC, few other kinesin-associated proteins (KAPs) have been identified. In many organisms, KHCs associate with various isoforms of kinesin-light chains (KLCs) to form complexes involved in transport of organelle and vesicle populations (Cyr et al., 1991; Beushausen et al., 1993; Gauger and Goldstein, 1993; Wedaman et al., 1993; Khodjakov et al., 1998; Rahman et al., 1998). Additionally, KHC has been shown to tightly associate with both a KLC kinase and a KLC phosphatase that putatively regulate motor function (McIlvain et al., 1994; Lindesmith et al., 1997). Two KAPs that interact with specific KRPs have also been identified. The KIF3 heterodimeric class of KRPs, also known as kinesin-II, interact with a single KAP to form a heterotrimeric complex (Cole et al., 1993, 1998; Scholey, 1996; Wedaman et al., 1996; Yamazaki et al., 1996). Finally, a *Saccharomyces cerevisiae* KRP, Kar3p, has been shown to associate with the Cik1 protein, which is essential for Kar3p localization and function during mating (Page et al., 1994).

The Kar3 protein is one of six KRPs encoded by the *S. cerevisiae* genome (Meluh and Rose, 1990). *KAR3* encodes a protein containing a kinesin-motor domain at its COOH terminus (Meluh and Rose, 1990). The Kar3p-motor domain possesses minus-end directionality and microtubule-depolymerizing activity in vitro (Endow et al., 1994). In addition to an essential role in nuclear fusion during mating, or karyogamy, Kar3p has been implicated in several microtubule functions during the vegetative cell cycle. These putative functions include spindle assembly, mitotic chromosome segregation, microtubule depolymerization, kinetochore-motor activity, spindle positioning, and as a force opposing the action of other KRPs (Meluh and Rose, 1990; Roof et al., 1991; Saunders and Hoyt, 1992; Hoyt et al., 1993; Endow et al., 1994; Middleton and Carbon, 1994; Cottingham and Hoyt, 1997; DeZwaan et al., 1997; Saunders et al., 1997a,b; Huyett et al., 1998). This presents an interesting problem: how can one motor protein perform such a diverse array of functions within a single cell?

The role of Cik1p during mating is to target Kar3p to cytoplasmic microtubules (Meluh and Rose, 1990; Page et al., 1994). Kar3p and Cik1p are interdependent for their localization to the SPBs and cytoplasmic microtubules of cells treated with mating pheromone (Page et al., 1994). Expression of *KAR3* and *CIK1* is increased upon exposure to pheromone, but both genes are also expressed during vegetative growth (Meluh and Rose, 1990; Page and Snyder, 1992; Kurihara et al., 1996). Cik1p is also involved in a subset of Kar3p's vegetative functions. *kar3Δ* and *cik1Δ* mutants share several vegetative phenotypes, including a growth defect at 37°C, enhanced cytoplasmic microtubules, very short mitotic spindles, and an accumulation of large budded cells indicative of a mitotic cell-cycle checkpoint delay (Meluh and Rose, 1990; Page and Snyder, 1992; Page et al., 1994). They also share genetic interactions with several genes (Manning et al., 1997). Furthermore, Cik1p requires Kar3p for its mitotic spindle localization (Page et al., 1994), and the two proteins coimmunoprecipitate from vegetative cell lysates (Barrett, J.G., B.D. Manning, and M. Snyder, unpublished data).

However, unlike during mating, Kar3p does not require Cik1p for its localization to the spindle poles in mitosis (Page et al., 1994; this study). This suggests that Kar3p has some Cik1p-independent functions. Genetic studies support this hypothesis. Kar3p is believed to oppose the force generated by two other *S. cerevisiae* KRPs, Cin8p and Kip1p, which are involved in spindle pole separation both during spindle assembly and during anaphase B spindle elongation (Hoyt et al., 1992, 1993; Roof et al., 1992; Saunders and Hoyt, 1992; Saunders et al., 1995). Disruption of *KAR3* function partially rescues the temperature-sensitive growth defect and spindle collapse phenotype of *cin8^{ts} kip1Δ* mutants (Saunders and Hoyt, 1992; Hoyt et al., 1993). In contrast, disruption of *CIK1* does not rescue this mutant (Page et al., 1994; this study). Together, these results suggest that Kar3p may perform some of its vegetative functions alone or in association with a different KAP.

In this study we describe a Cik1p-homologous protein in *S. cerevisiae* that acts as a second KAP for Kar3p. We demonstrate that this protein, Vik1p (vegetative interaction with Kar3p), is present in vegetatively growing cells but absent from mating-pheromone treated cells. Vik1p forms a complex with Kar3p that is distinct from that between Kar3p and Cik1p. Furthermore, we show that Kar3p and Vik1p are interdependent for their concentration at the poles of the mitotic spindle. Phenotypic and genetic comparisons of *cik1Δ* and *vik1Δ* mutants demonstrate that Cik1p and Vik1p are likely to mediate distinct subsets of Kar3p functions. Our data suggest that Cik1p and Vik1p regulate Kar3p function, at least in part, by targeting the motor to various sites of action within the cell. This is the first example of two distinct associated proteins differentially regulating a single KRP.

Materials and Methods

Strains, Media, and Standard Methods

S. cerevisiae strains used in this study are listed in Table I. Yeast growth media, molecular biological techniques, and genetic manipulations were as described previously (Sambrook et al., 1989; Guthrie and Fink, 1991). Yeast transformation procedures were performed using the lithium acetate method (Ito et al., 1983). Where indicated, rich medium, consisting of yeast extract, peptone, and dextrose, was supplemented with benomyl (DuPont), dissolved in DMSO, to a final concentration of 10, 20, or 30 μg/ml. Sensitivity of wild-type yeast strains to these concentrations of benomyl varied between preparations of benomyl containing agar plates and, hence, growth comparisons were always performed on the same plate. Sensitivity also varies dramatically between growth temperatures (i.e., at 23°C strains are much more benomyl sensitive than at 30°C).

Construction of *VIK1*::3XHA Strain

A strain containing the *VIK1*::*3XHA* allele (Y1744) was constructed by the PCR-epitope tagging method described previously (Schneider et al., 1995). The primers 5′-TATTAACGATTTCAGAAGAAGTTCAAACACAACTTTGTAAAAGAAAGAAAAAGCTCACTAGGGAACAAAAAGCTGG-3′ and 5′-CTTATTTGTTTCATATCTAAATGGCTGTGTTAAGAAAGACGATAATGTGACCGAGCTTACTATAGGGCGAATTGG-3′ were used in a PCR reaction with pMPY-3XHA as the template. The resulting 1.5-kb PCR product contains the *URA3* gene flanked by direct repeats encoding three copies of the hemagglutinin (HA) epitope and contains 59 bp of sequence from the 3′ end of the *VIK1* gene at one end and 59 bp of sequence downstream of, and including, the *VIK1* translation termination codon at the other end. This fragment was

Table I. Strain List

Strain	Genotype
Y270	*MATa/MATα ura3-52/ura3-52 lys2-801/lys2-801 ade2-101/ade2-101 trp1-Δ1/trp1-Δ1 his3-Δ200/his3-Δ200*
Y817	*MATa ura3-52 ade2-101 leu2-3,112 his3-Δ200 cin8-3 kip1Δ::HIS3*
Y818	*MATα ura3-52 ade2-101 leu2-3,112 his3-Δ200 cin8-3 kip1Δ::HIS3*
Y1707	*MATα ura3-52 lys2-801 ade2-101 trp1-Δ1 his3-Δ200 cik1Δ::TRP1*
Y1731	*MATa ura3-52 lys2-801 ade2-101 leu2-98 trp1-Δ1 his3-Δ200*
Y1733	*MATa/MATα ura3-52/ura3-52 lys2-801/lys2-801 ade2-101/ade2-101 trp1-Δ1/trp1-Δ1 his3-Δ200/his3-Δ200 vik1Δ::HIS3-Km^r/VIK1*
Y1734*	*MATa ura3-52 lys2-801 ade2-101 trp1-Δ1 his3-Δ200 vik1Δ::HIS3-Km^r*
Y1738‡	*MATa/MATα ura3-52/ura3-52 lys2-801/lys2-801 ade2-101/ade2-101 trp1-Δ1/trp1-Δ1 his3-Δ200/his3-Δ200 vik1Δ::HIS3-Km^r/VIK1 cik1-Δ3::TRP1/CIK1*
Y1744	*MATa ura3-52 lys2-801 ade2-101 leu2-98 trp1-Δ1 his3-Δ200 VIK1::3XHA*
Y1745	*MATa ura3-52 lys2-801 ade2-101 leu2-98 trp1-Δ1 his3-Δ200 cik1-Δ3::LEU2 VIK1::3XHA*
Y1748	*MATα ura3-52 ade2-101 leu2-3,112 his3-Δ200 cin8-3 kip1Δ::HIS3 vik1Δ::URA3-Km^r*
Y1750	*MATa ura3-52 lys2-801 ade2-101 leu2-98 trp1-Δ1 his3-Δ200 kar3-Δ4::URA3 VIK1::3XHA*
Y1751§	*MATα ura3-52 leu2-98 his3-Δ200 cik1Δ::LEU2 KAR3::HAT*
Y1752	*MATa ura3-52 leu2-98 his3-Δ200 can^r vik1Δ::HIS3-Km^r KAR3::HAT*
Y1753‖	*MATa/MATα ura3-52/ura3-52 leu2-98/leu2-98 his3-Δ200/his3-Δ200 vik1Δ::HIS3-Km^r/VIK1 cik1Δ::LEU2/CIK1 KAR3::HAT/KAR3::HAT*
Y1758	*MATa ura3-52 ade2-101 leu2-3,112 his3-Δ200 cin8-3 kip1Δ::HIS3 cik1-Δ3::LEU2*
Y1759	*MATα ura3-52 ade2-101 leu2-3,112 his3-Δ200 cin8-3 kip1Δ::HIS3 kar3-Δ4::URA3*
Y1864	*MATα ura3-52 leu2-98 trp1-Δ1 cik1Δ::LEU2*
Y1869	*MATa ura3-52 leu2-98 his3-Δ200 can^r* plus pB227
Y1870	*MATa ura3-52 leu2-98 his3-Δ200 can^r KAR3::HAT*
Y1871¶	*MATa/MATα ura3-52/ura3-52 leu2-98/leu2-98 his3-Δ200/his3-Δ200 cik1Δ::LEU2/CIK1 KAR3::HAT/KAR3*

*Y1733 segregant.
‡Y1707 × Y1734.
§Y1871 segregant.
‖Y1751 × Y1752.
¶Y1864 × Y1870.

used to transform yeast strain Y1731, and transformants were selected on synthetic complete medium lacking uracil. Correct integration into the 3′ region of the *VIK1* locus was confirmed by PCR analysis with primers to sequences flanking the site of insertion. Transformants with a correct *3XHA-URA3-3XHA* integration were then incubated on plates containing 5-fluoroorotic acid to select for loss of the *URA3* marker by recombination between the repeated *3XHA* regions. The resulting *VIK1::3XHA* allele was confirmed by PCR and immunoblot analysis. This allele does not display any *vik1Δ* phenotypes; growth of *VIK1::3XHA* strains in the presence of benomyl is identical to wild-type strains, and the temperature-sensitive growth defect of *cik1Δ* mutants is the same in a *VIK1* or *VIK1::3XHA* background.

Immunoprecipitations and Immunoblot Analysis

Cells were grown in rich liquid medium to mid-logarithmic phase (OD_{600} = 0.5–0.8), and a total of 10 OD_{600} units of cells were collected by centrifugation, washed, and resuspended in 100 μl lysis buffer (1 M NaCl, 10 mM EDTA, 2 mM EGTA, 5% glycerol, 40 mM Tris-HCl, pH 7.5, containing 1 μl yeast protease inhibitor cocktail (Sigma Chemical Co.) and 200 μM PMSF). When indicated, cells were first washed twice with fresh medium, resuspended in medium containing 5 μg/ml α-factor mating pheromone (Sigma Chemical Co.), and incubated for 2 h before harvesting. Cell lysates were prepared in Eppendorf tubes using zirconia/silica beads (Biospec Products) with 40-s pulses of vortexing separated by incubations on ice; this procedure was repeated 6–8 times. Lysates were then centrifuged for 10 min at 6,500 *g*, and a 10-μl aliquot was removed for immunoblot analysis.

For immunoprecipitations, the remaining cell lysate and beads were washed with 500 μl lysis buffer containing detergents (1% NP-40, 0.5% sodium deoxycholate, and 0.1% SDS) without NaCl for 20 min on a roller drum at 4°C. Lysates were then cleared of unlysed cells and cell debris by centrifugation for 10 min at 6,500 *g* and ~500 μl of supernatant was transferred to a new tube. The 500 μl lysate was brought to a 1-ml vol with the same lysis buffer plus detergents (100 mM final NaCl concentration). The cell lysate was then precleared for 1 h by incubation with 20 μl of a 1:1 slurry of protein A/G–agarose (Pierce) and TBS (150 mM NaCl, 50 mM Tris-HCl, pH 8.0). Immunoprecipitations were performed by incubation of cell lysates with either 2 μl mouse monoclonal anti-HA antibodies (12CA5 from BABCO), 10 μl rabbit polyclonal anti-Cik1p antibodies (Page and Snyder, 1992), or 5 μl rabbit polyclonal anti-Kar3p antiserum (gift of L.L. Satterwhite, P.B. Meluh, and M.D. Rose, Princeton University, Princeton, NJ; Meluh and Rose, 1990; Page et al., 1994) for 2 h. 20 μl protein A/G–agarose was then added and incubated for 1 h before collection by centrifugation at 2,000 *g* for 1 min. The protein A/G–agarose antibody complexes were then washed twice with 1 ml TBS containing detergents and protease inhibitors (1% NP-40, 0.5% sodium deoxycholate, 0.1% SDS, 1 μl Sigma yeast protease inhibitor cocktail, 200 mM PMSF) and once with 1 ml TBS plus protease inhibitors. The final pellet was resuspended in 30 μl Laemmli sample buffer (Laemmli, 1970).

Proteins from cell lysates and immunoprecipitations were denatured by incubation at 90°C for 10 min before electrophoretic separation in either 8% or 10% SDS–polyacrylamide gels. For attempts to detect Vik1p-3XHA in mating-pheromone treated cells, a threefold larger volume of cell lysate was loaded than for vegetative cell lysates (data not shown). Proteins were then transferred to Immobilon-P membranes (Millipore) for immunoblot analysis with either mouse monoclonal anti-HA antibodies (12CA5 from BABCO), rabbit polyclonal anti-Cik1p antibodies (Page and Snyder, 1992), or a crude IgG fraction of the rabbit polyclonal anti-Kar3p antiserum (Meluh and Rose, 1990; Page et al., 1994). Reactive protein bands were then detected with alkaline phosphatase-conjugated secondary antibodies (Amersham) and the CDP Star detection reagent (Boehringer Mannheim). Overexposure of all blots failed to detect Vik1p-3XHA in cell lysates from mating-pheromone treated cells.

Fluorescence Microscopy

Indirect immunofluorescence was performed as described previously (Gehrung and Snyder, 1990; Pringle et al., 1991). Due to sensitivity of the HA-epitope to formaldehyde fixation, mid-logarithmic phase cells were fixed with 3.7% formaldehyde for only 15 min. They were then washed twice with solution A (1.2 M sorbitol, 50 mM potassium phosphate buffer, pH 6.8), and spheroplasts were prepared by incubating cells in solution A containing 5 μg/ml Zymolyase 100T, 0.03% glusulase, and 0.2% 2-mercaptoethanol at 37°C for 15 to 30 min. Spheroplasted cells were then washed and resuspended in solution A and placed onto poly(L-lysine)-coated slides. Vik1p-3XHA and Kar3p-HAT were detected by incubation overnight at 4°C with preabsorbed mouse monoclonal anti-HA primary

antibodies (16B12 from BABCO) diluted in PBS/BSA. Bound mouse anti-HA antibodies were then detected by incubation for 90 min at room temperature with preabsorbed CY3-conjugated goat anti-mouse secondary antibodies (Jackson ImmunoResearch Laboratory, Inc.). Microtubules were detected by incubation with rabbit anti-yeast β-tubulin (Tub2p) primary antibodies (gift of F. Solomon, Massachusetts Institute of Technology; Bond et al., 1986) followed by incubation with FITC-conjugated goat anti–rabbit secondary antibodies. After both primary and secondary antibody incubations, slides were washed twice with PBS/BSA and twice with PBS/BSA plus 0.1% NP-40. Finally, slides were mounted in 70% glycerol, 2% *n*-propyl gallate, and 0.25 μg/ml Hoechst 33258 to preserve the preparation and stain DNA for localization of nuclei.

Photographs of representative cells stained with anti-HA antibodies, anti-Tub2p antibodies, and/or Hoechst 33258 were taken, and composite figures were produced and processed using Adobe Photoshop version 3.0 (Adobe Systems, Inc.). Processing procedures were identical for each photo of a particular staining method within a composite figure.

Construction of KAR3::HAT Strains

A strain containing the *KAR3::HAT* allele was constructed using a transposon insertion technique described previously (Ross-MacDonald et al., 1997). The entire *KAR3* coding region was cloned into the vector pHSS6 and subjected to transposon mutagenesis in *Escherichia coli* as described (Ross-MacDonald et al., 1997). Plasmid DNA was prepared from selected strains and digested with NotI, producing a fragment containing the mTn-3xHA/*lacZ* transposon inserted randomly into the *KAR3* gene. These fragments were then used to transform yeast strain Y1869, using the *URA3* marker encoded by the transposon for selection. Transformants with in-frame transposon insertions into the *KAR3* genomic locus were selected by detection of β-galactosidase activity as described (Burns et al., 1994). Cre recombinase-mediated excision, leaving only the 93 amino acid HA/transposon tag (HAT) inserted, was induced by growth on galactose (pB227 contains *cre* under control of a galactose-inducible promoter). Recombinants were selected on 5-fluoroorotic acid. Strains with in-frame HAT insertions were then tested for *kar3Δ* mutant phenotypes, such as defects in karyogamy and temperature sensitivity. PCR and sequence analysis was performed on DNA from fully complementing strains in order to determine the site of insertion within the *KAR3* gene.

Strain Y1870 contains a *KAR3* allele with a *HAT* insertion after the codon for S^{68}, and does not exhibit any *kar3Δ* phenotypes. Y1870 was then crossed with Y1864 to yield Y1871. Y1871 was then sporulated and a *MATα KAR3::HAT cik1Δ::LEU2* segregant (Y1751) was isolated. The *VIK1* gene was disrupted with the *HIS3* marker in Y1870 yielding Y1752 (see below). Y1752 was then crossed with Y1751 yielding Y1753. Y1753 haploid segregants were used to analyze Kar3p-HAT localization in wild-type, *cik1Δ*, *vik1Δ*, and *cik1Δ vik1Δ* strains.

Cloning of VIK1 and Disruption of VIK1, CIK1, and KAR3

Sequence of the *VIK1* gene was acquired from the *Saccharomyces* Genome Database (ORF designation YPL253c; Stanford University). A 2,920-bp region, from the MscI site 5′ of the predicted *VIK1* translation start site to the SpeI site 3′ of the *VIK1* translation termination site, was PCR amplified from yeast genomic DNA and cloned into pBluescript SK (Stratagene), replacing its EcoRV-SpeI fragment (pSK-*VIK1*). The SalI-SacII fragment from this plasmid, containing the *VIK1* gene and flanking sequences, was cloned into the SalI-SacII site of the CEN plasmid pRS316 (Sikorski and Hieter, 1989). This plasmid was linearized by deleting the NruI-AflII fragment containing the entire *VIK1* ORF, then gap repaired in a wild-type yeast strain (Guthrie and Fink, 1991). This CEN plasmid encoding wild-type *VIK1* was used for subsequent phenotypic analysis.

VIK1 disruption constructs were made by replacing the NruI-AflII fragment of pSK-*VIK1* with the SmaI fragment from either pJA50 (*HIS3-Km*^{r}) or pJA53 (*URA3-Km*^{r}) (Elledge and Davis, 1988). SalI-XbaI fragments from these plasmids, containing either the *HIS3* or *URA3* selectable markers flanked by the 5′ and 3′ noncoding regions of *VIK1*, were used to transform yeast strains Y270, Y818, and Y1870 yielding *vik1Δ* strains Y1733, Y1748, and Y1752, respectively.

CIK1 and *KAR3* disruptions were made as previously described (Page and Snyder, 1992; Page et al., 1994). The *cik1-Δ3::LEU2* construct was used to transform strains Y817 and Y1744 yielding *cik1Δ* strains Y1758 and Y1745, respectively. The *kar3-Δ4::URA3* construct was used to transform strains Y818 and Y1744 yielding *kar3Δ* strains Y1759 and Y1750, respectively.

Results

Vik1p: A Cik1p Homologue Present in Vegetative Cells but Not in Cells Treated with Mating Pheromone

A database homology search with the Cik1p amino acid sequence identified an open reading frame (ORF) on chromosome XVI of the *S. cerevisiae* genome (BLAST search of predicted translation products of *S. cerevisiae* ORFs; *Saccharomyces* Genome Database ORF designation YPL253c) predicted to encode a protein with significant homology to Cik1p. This gene was named *VIK1*, for vegetative interaction with Kar3p (see below). *VIK1* is predicted to encode a protein of 647 amino acids, with an overall sequence identity of 24%, and similarity of 37%, to Cik1p. The Vik1p sequence also shares structural similarity to Cik1p. It contains a predicted α-helical coiled-coil domain (amino acids 80–385) of the same length and location as that found in Cik1p (amino acids 81–388; Page and Snyder, 1992; Fig. 1; predicted with COILS version 2.2; Lupas et al., 1991; Lupas, 1996); both proteins contain a short break of 40 amino acids in their coiled-coil regions. This break and an 80 residue NH_2-terminal globular domain are the most divergent regions of the two proteins (16% identity). One notable difference in the amino terminal domain is that Vik1p lacks a recognizable nuclear localization signal found in Cik1p (amino acids 24 to 33; Fig. 1; Barrett, J.G., and M. Snyder, manuscript in preparation). Finally, the COOH-terminal globular domains of the two proteins share two regions of 134 and 43 amino acids in length with 25% identity each. Therefore, Vik1p shares sequence and structural homology to Cik1p which is not confined to their coiled-coil domains.

To characterize the Vik1 protein by immunoblot and immunofluorescence analysis, DNA encoding a triple HA-epitope tag was integrated into the COOH-terminal coding region of the *VIK1* genomic locus (see Materials and Methods). The resulting *VIK1::3XHA* fusion allele fully complements *VIK1* function (see Materials and Methods). Immunoblot analysis using anti-HA monoclonal antibodies detects a protein of 92-kD in cell lysates and anti-HA immunoprecipitations from *VIK1::3XHA* strains (Fig. 2 A). This molecular mass is close to the predicted 76-kD of Vik1p plus the triple-HA epitope tag. This fusion protein is not detected in cell lysates or anti-HA immunoprecipitations from *VIK1* untagged strains (Fig. 2 A). Therefore, the *VIK1::3XHA* allele is expressed during vegetative growth and produces a functional protein of the expected size.

The Vik1p-3XHA protein is not detected in cell lysates or anti-HA immunoprecipitations from cultures first exposed to the α-factor mating pheromone (Fig. 2 A; see Materials and Methods). In contrast, Cik1p greatly increases in abundance upon exposure to α-factor (Fig. 2 B; Page and Snyder, 1992). Consistent with this result, the region upstream of the *VIK1* ORF does not contain any predicted pheromone-response elements (Kronstad et al., 1987). However, the pheromone-inducible *CIK1* and *KAR3* genes each contain multiple pheromone-response

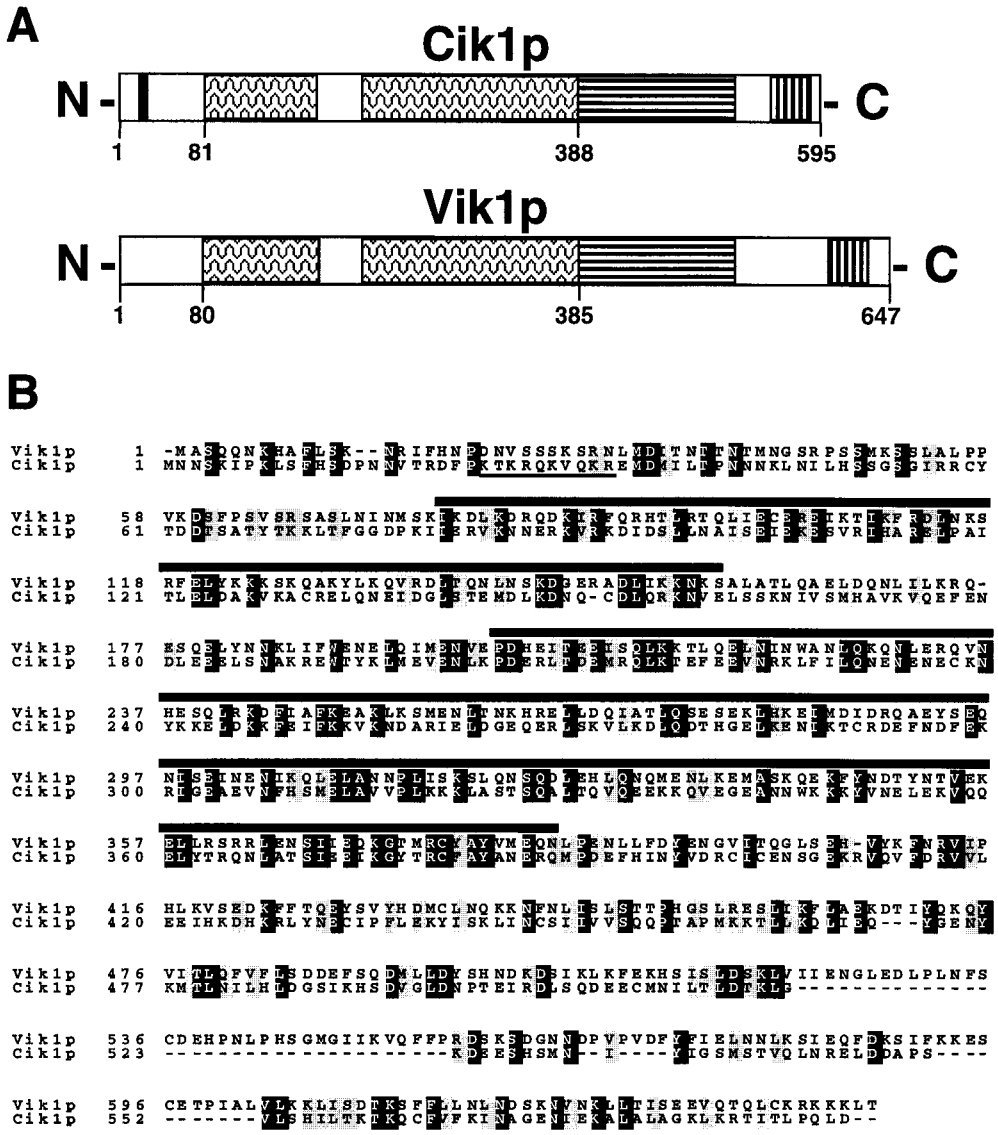

Figure 1. Vik1p is a homologue of Cik1p. (A) Schematic representation of Cik1p and Vik1p. Regions with the same shading pattern between the two proteins share at least 25% amino acid sequence identity. The two proteins have homologous regions predicted to form α-helical coiled-coil structures (wavy line shading), as well as two other stretches of homology in their carboxyl termini (horizontal and vertical line shading). Cik1p contains a nuclear localization signal at its NH_2 terminus (black box). (B) Amino acid sequence alignment of Vik1p and Cik1p. Identical and similar residues are indicated by dark and light shading, respectively. The predicted coiled-coil regions of the two proteins are denoted by a black bar over the sequence, whereas the nuclear localization signal of Cik1p is underlined. The alignment was performed with BCM Search Launcher: Multiple Sequence Alignments (Baylor College of Medicine, Houston, TX). Shading was performed by the Boxshade 3.21 program (ISREC Bioinformatics Group).

elements in their 5′ noncoding regions (Meluh and Rose, 1990; Page and Snyder, 1992). Thus, since Vik1p is not present during mating-pheromone induced differentiation, it is not likely to have a significant role during mating.

Vik1p Coimmunoprecipitates with Kar3p

Cik1p physically associates with Kar3p (Page et al., 1994), and Vik1p shares sequence and structural similarity to Cik1p; we therefore tested whether Vik1p could also interact with Kar3p. Cell lysates were prepared from wild-type, *kar3Δ*, and *cik1Δ* strains expressing either the *VIK1::3XHA* allele or untagged *VIK1*. Proteins from these cell lysates were separated by SDS-PAGE (Fig. 3 A) or first immunoprecipitated with anti-Kar3p polyclonal antibodies (Fig. 3 B; Meluh and Rose, 1990; Page et al., 1994). Immunoblot analysis using anti-HA antibodies detects Vik1p-3XHA in cell lysates from wild-type, *kar3Δ*, and *cik1Δ* strains containing the *VIK1::3XHA* allele but not in untagged strains (Fig. 3 A). Therefore, Vik1p stability is not affected by the absence of either Kar3p or Cik1p. Anti-HA immunoblots of proteins immunoprecipitated with anti-Kar3p antibodies detects Vik1p-3XHA from a wild-type *VIK1::3XHA* strain but not from a *kar3Δ VIK1::3XHA* strain or an untagged strain (Fig. 3 B). Therefore, immunoprecipitation data indicate that Kar3p and Vik1p physically interact. Furthermore, the Kar3p-Vik1p complex is quite stable, as cell lysates were prepared in a 1 M NaCl solution (see Materials and Methods).

Vik1p-3XHA is also detected in anti-Kar3p immunoprecipitations from a *cik1Δ VIK1::3XHA* strain (Fig. 3 B), indicating that Cik1p is not required for this interaction between Kar3p and Vik1p. Furthermore, an association between Vik1p and Cik1p is not detected by immunoprecipitation experiments. Vik1p-3XHA is not precipitated from *VIK1::3XHA* cell lysates by anti-Cik1p polyclonal antibodies (Fig. 2 A; Page and Snyder, 1992; Page et al., 1994), and, reciprocally, Cik1p is not precipitated from these cell lysates with anti-HA antibodies (Fig. 2 B). Protein preparations from vegetatively growing cells or α-fac-

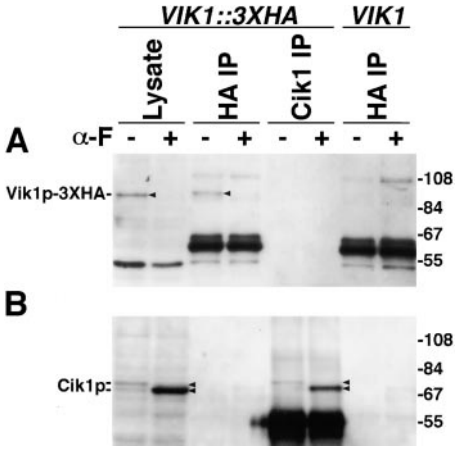

Figure 2. Vik1p is not present in mating pheromone-treated cells and does not coimmunoprecipitate with Cik1p. Cell lysates were prepared from a *VIK1::3XHA* strain (Y1744) and a *VIK1* untagged strain (Y1731) that were either grown vegetatively (α-F −) or first exposed to the α-factor mating pheromone (α-F +). Proteins from these lysates were either separated by SDS-PAGE using a 10% gel (Lysate) or first immunoprecipitated with anti-HA antibodies (HA IP) or anti-Cik1p antibodies (Cik1 IP) before SDS-PAGE separation. (A) Immunoblot analysis with anti-HA antibodies detects a protein of 92 kD in *VIK1::3XHA* cell lysates and anti-HA immunoprecipitations from vegetative cells, but not from α-factor treated cells, anti-Cik1p immunoprecipitations, or *VIK1* anti-HA immunoprecipitations. (B) Immunoblot analysis with anti-Cik1p antibodies detects the 73–77-kD Cik1 protein in *VIK1::3XHA* cell lysates and anti-Cik1p immunoprecipitations from both vegetative and α-factor treated cells, but not from *VIK1::3XHA* or *VIK1* anti-HA immunoprecipitations. The mass of molecular mass markers are shown in kilodaltons.

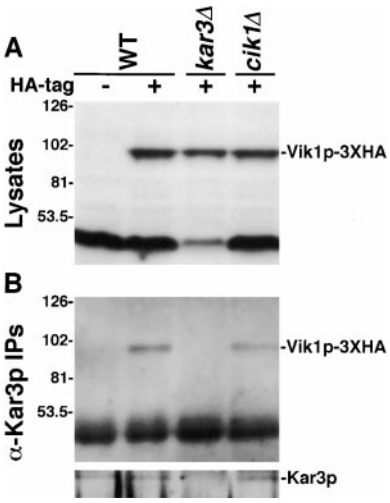

Figure 3. Vik1p coimmunoprecipitates with Kar3p. Cell lysates were prepared from vegetatively growing cultures of a wild-type (WT) *VIK1* untagged strain (Y1731; HA-tag −) and wild-type (Y1744), *kar3Δ* (Y1750), and *cik1Δ* (Y1745) *VIK1::3XHA* strains (HA-tag +). Proteins from these lysates were either separated by SDS-PAGE using an 8% gel (A; Lysates) or first immunoprecipitated with anti-Kar3p antibodies (B; α-Kar3p IPs) before SDS-PAGE separation. (A) Immunoblot analysis with anti-HA antibodies detects the 92 kD Vik1-3XHA protein in cell lysates from the wild-type, *kar3Δ*, and *cik1Δ VIK1::3XHA* strains, but not from the *VIK1* untagged strain. (B, top) Immunoblot analysis with anti-HA antibodies detects Vik1p-3XHA in anti-Kar3p immunoprecipitations from the wild-type and *cik1Δ VIK1::3XHA* strains, but not from the *VIK1* untagged strain or the *kar3Δ VIK1::3XHA* strain (B, bottom). Immunoblot analysis with anti-Kar3p antibodies detects the 88 kD Kar3 protein in anti-Kar3p immunoprecipitations from the wild-type *VIK1* untagged strain and wild-type and *cik1Δ VIK1::3XHA* strains, but not from the *kar3Δ VIK1::3XHA* strain (B, bottom). The mass of molecular mass markers are shown in kilodaltons.

tor–treated cells produce the same results. Thus, Vik1p and Cik1p do not appear to be part of the same complex. Together, these results suggest that Vik1p and Cik1p interact with Kar3p separately, and, therefore, form two different complexes during vegetative growth.

Vik1p Localizes to the Spindle-Pole Bodies

To determine the subcellular localization of Vik1p, asynchronous cultures of *VIK1::3XHA* and *VIK1* untagged strains were fixed briefly with formaldehyde and analyzed by immunofluorescence using anti-HA and anti-tubulin antibodies (see Materials and Methods). *VIK1::3XHA* cells display anti-HA staining concentrated at the yeast microtubule-organizing centers, or spindle-pole bodies (SPBs), in all stages of the cell cycle (Fig. 4, B and C). The position of the SPBs correspond to the brightest foci of anti-tubulin staining. Anti-HA staining at the SPBs is not detected in *VIK1* untagged cells (Fig. 4 A). Moreover, detection of Vik1p-3XHA at the SPBs does not require costaining with anti-tubulin antibodies; staining of dots at the edges of both preanaphase and anaphase nuclei is still observed in control cells not stained with anti-tubulin antibodies (Fig. 4 C). Vik1p-3XHA staining is brightest in preanaphase cells with short spindles, where localization is clearly concentrated at the spindle poles (pattern observed in 100% of preanaphase spindles; $n > 200$; Fig. 4 B). Cells in the G1 phase of the cell cycle, scored as unbudded cells with a single SPB, display SPB staining that is more faint and not observed in every cell (staining observed in 60% of G1 cells; $n = 100$). Finally, cells in early or late anaphase, as scored by elongated spindles and/or elongated nuclei penetrating the bud neck, display faint staining concentrated at the spindle poles (staining of at least one spindle pole is observed in 73% of anaphase cells; $n = 100$; Fig. 4 C, inset). Anti-HA staining is not detected along the lengths of spindle or cytoplasmic microtubules in *VIK1::3XHA* cells. Short fixation times due to sensitivity of the HA-epitope to formaldehyde leads to a diminished number of cytoplasmic microtubules. However, in cells that contain cytoplasmic microtubules, only staining at the SPBs is observed; microtubule staining is not evident. These staining patterns are independent of ploidy, and the nature and position of the epitope tag. *VIK1::3XHA/VIK1::3XHA* homozygous diploids, and cells expressing a *VIK1::3Xmyc* NH_2-terminal fusion allele stained with anti-myc monoclonal antibodies, exhibit identical patterns to those found in *VIK1::3XHA* haploid cells (data not shown).

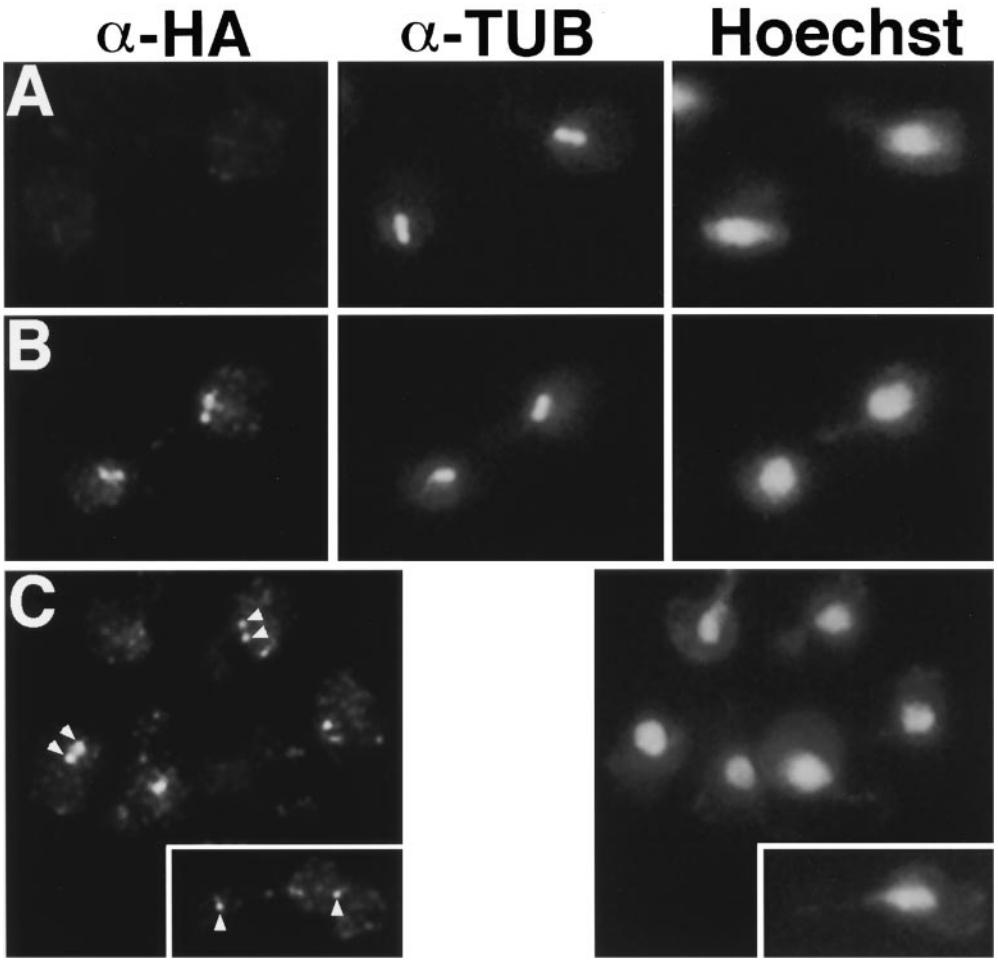

Figure 4. Vik1p localizes to the spindle-pole bodies. Cells from growing cultures of *VIK1* untagged strain Y1731 (A) and *VIK1::3XHA* strain Y1744 (B) were prepared for indirect immunofluorescence microscopy using anti-HA antibodies (A–C, left), anti-Tub2p antibodies (A and B, middle), and Hoechst 33258 staining (A–C, right). Representative cells are pictured: (A) two cells with preanaphase spindles from the *VIK1* untagged strain demonstrating background staining; (B) two cells with preanaphase spindles from the *VIK1::3XHA* strain displaying Vik1p-3XHA staining at the spindle poles; (C) a field of *VIK1::3XHA* cells from a preparation not stained with anti-Tub2p antibodies, demonstrating that Vik1p-3XHA localization to one or two dots at the nuclear periphery does not depend on costaining of microtubules. Presumptive spindle-pole staining of two preanaphase cells and one cell in anaphase (inset) is indicated (C, arrowheads). The portion of the nucleus that has entered the bud in the inset C cell is out of the plane of focus, but its periphery overlaps with the dot indicated by the arrowhead.

The localization of Vik1p at, or near, the SPBs at various levels throughout the vegetative cell cycle is very similar to that reported for fusion proteins of Kar3p with either β-galactosidase or HA (Page et al., 1994; Saunders et al., 1997; see below). However, in pheromone-treated cells, when Kar3p localizes to the SPB and cytoplasmic microtubules (Meluh and Rose, 1990; Page et al., 1994), Vik1p-3XHA staining above background is not detected (data not shown). This is consistent with immunoblot data demonstrating the absence of Vik1p in cell lysates from α-factor–treated cells (Fig. 2 A), and further suggests that Vik1p functions in vegetative cells, but not mating cells.

Spindle-Pole Body Localization of Vik1p is Kar3p Dependent

Since Kar3p and Vik1p physically associate and have similar localization patterns, we investigated whether the localization of Vik1p to the SPBs was dependent on the presence of Kar3p. Therefore, Vik1p-3XHA localization was analyzed by anti-HA immunofluorescence in *kar3Δ* cells. Whereas Vik1p-3XHA concentrates at the SPBs in wild-type cells, it does not localize to the SPBs at any stage of the cell cycle in the *kar3Δ* mutant. Instead, the protein is present in cytoplasmic patches that appear to be excluded from the nucleus (SPB staining was not detected in any cells; $n > 300$; a representative preanaphase cell is shown in Fig. 5 B). This pattern is also observed with anti-myc staining in *kar3Δ* cells containing the *VIK1::3Xmyc* allele (data not shown). These cytoplasmic patches are not detected in *kar3Δ VIK1* untagged strains (Fig. 5 A). SPB localization of Vik1p-3XHA can be restored by introducing a CEN plasmid containing *KAR3* into the *kar3Δ VIK1::3XHA* strain (Fig. 5 C). This plasmid also restores normal spindle length, since disruption of *KAR3* results in accumulation of cells with short spindles compared with wild-type cells (Meluh and Rose, 1990). Therefore, the Kar3p-Vik1p association is required for localization of Vik1p to the SPB.

Cik1p also localizes to the SPB in a Kar3p-dependent manner (Page et al., 1994), and, like *kar3Δ* mutants, *cik1Δ* mutants accumulate cells with short mitotic spindles (Page

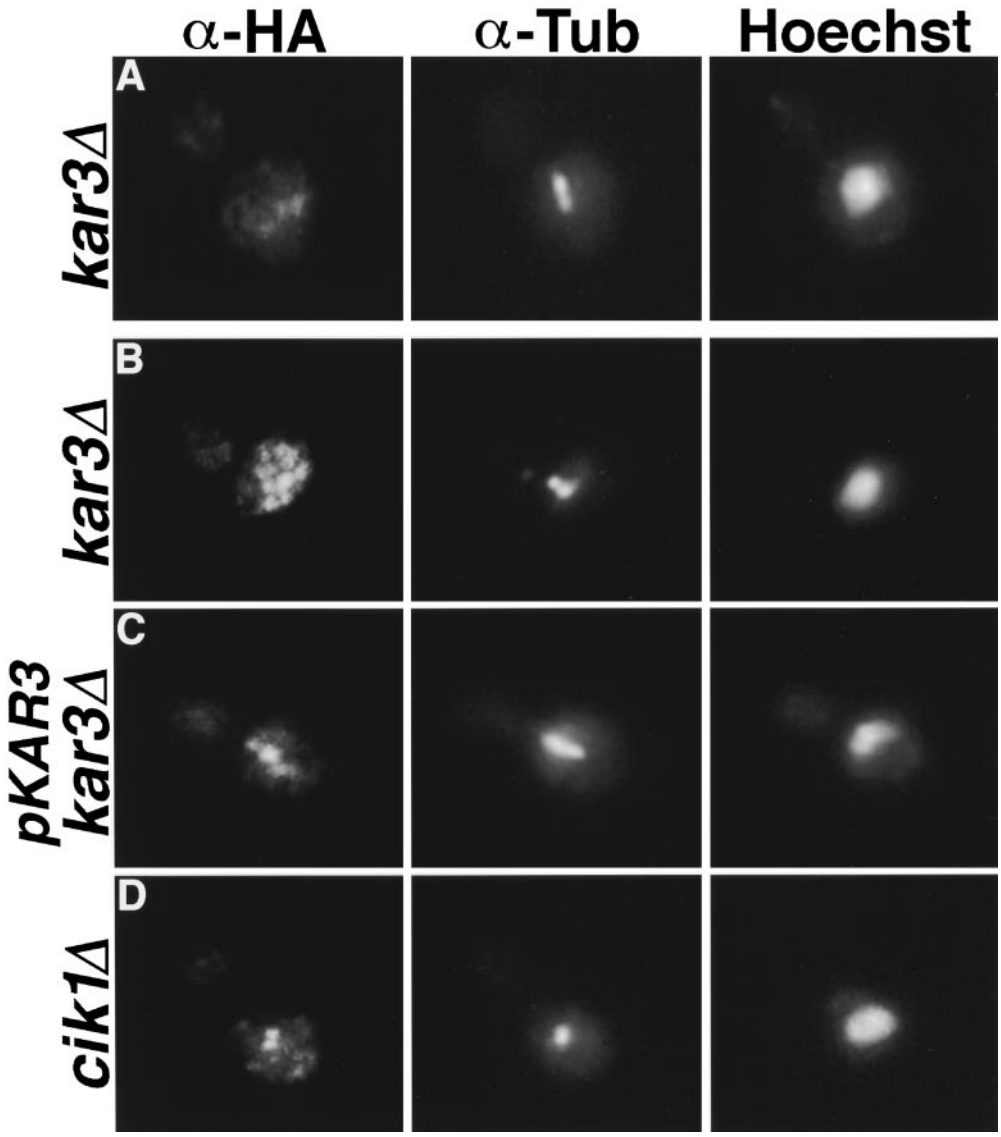

Figure 5. The spindle-pole body localization of Vik1p depends on Kar3p. Cells from growing cultures of a *kar3Δ VIK1* untagged strain (A), *kar3Δ VIK1::3XHA* strain Y1750 (B), Y1750 containing *KAR3* on a YCp50-derived CEN plasmid (C), and *cik1Δ VIK1::3XHA* strain Y1745 (D) were prepared for indirect immunofluorescence microscopy with anti-HA antibodies (left), anti-Tub2p antibodies (middle), and Hoechst 33258 staining (right). Representative preanaphase cells are pictured: (A) an untagged cell demonstrating background staining; (B) a cell displaying Vik1p-3XHA mislocalization to cytoplasmic patches in the absence of Kar3p; (C) restoration of Vik1p-3XHA spindle-pole localization by introduction of a wild-type copy of *KAR3*, and; (D) Vik1p-3XHA localization to the poles of a short spindle from a *cik1Δ* cell.

and Snyder, 1992). Therefore, in order to determine if Cik1p was involved in localizing Vik1p to the SPB or if the short spindle phenotype was responsible for Vik1p mislocalization in *kar3Δ* mutants, we analyzed Vik1p-3XHA localization in a *cik1Δ* mutant. In contrast to *kar3Δ* cells, *cik1Δ* cells display Vik1p-3XHA staining concentrated at the SPBs during all stages of the cell cycle, as observed in wild-type cells. Furthermore, HA staining is brightest at the poles of the short preanaphase spindles present in *cik1Δ* cells (a representative cell is shown in Fig. 5 D), indicating that the short spindle phenotype alone is not the cause of mislocalization of Vik1p. Therefore, these immunolocalization data support the immunoprecipitation experiments; Vik1p does not appear to be part of the same complex as Cik1p. Furthermore, Vik1p localization to the SPBs does not require Cik1p function.

Proper Spindle-Pole Body Localization of Kar3p in Vegetative Cells Is Vik1p Dependent

Cik1p is required to localize Kar3p to the SPB and cytoplasmic microtubules during mating but is not required for Kar3p localization to the mitotic spindle poles (Page et al., 1994). This suggests that in vegetative cells, Kar3p can either target to the SPBs by itself or interacts with another protein that is responsible for its concentration at the SPBs. Based on its localization and association with Kar3p, Vik1p could fulfill this function. Therefore, Kar3p was localized in the absence of Vik1p, Cik1p, and both Vik1p and Cik1p.

The subcellular localization pattern of Kar3p has been determined previously using fusion proteins that do not fully complement all of the *kar3Δ* phenotypes (Meluh and Rose, 1990; Page et al., 1994; Saunders et al., 1997). To create a fully complementing HA epitope-tagged version of Kar3p, we used a transposon insertion technique described previously (Ross-MacDonald et al., 1997; see Materials and Methods). Using this technique we created several strains containing in-frame insertions of the HAT into random regions of the *KAR3* genomic locus. We then tested these strains for several *kar3Δ* phenotypes, such as defects in karyogamy and meiosis, slow growth, temperature-sen-

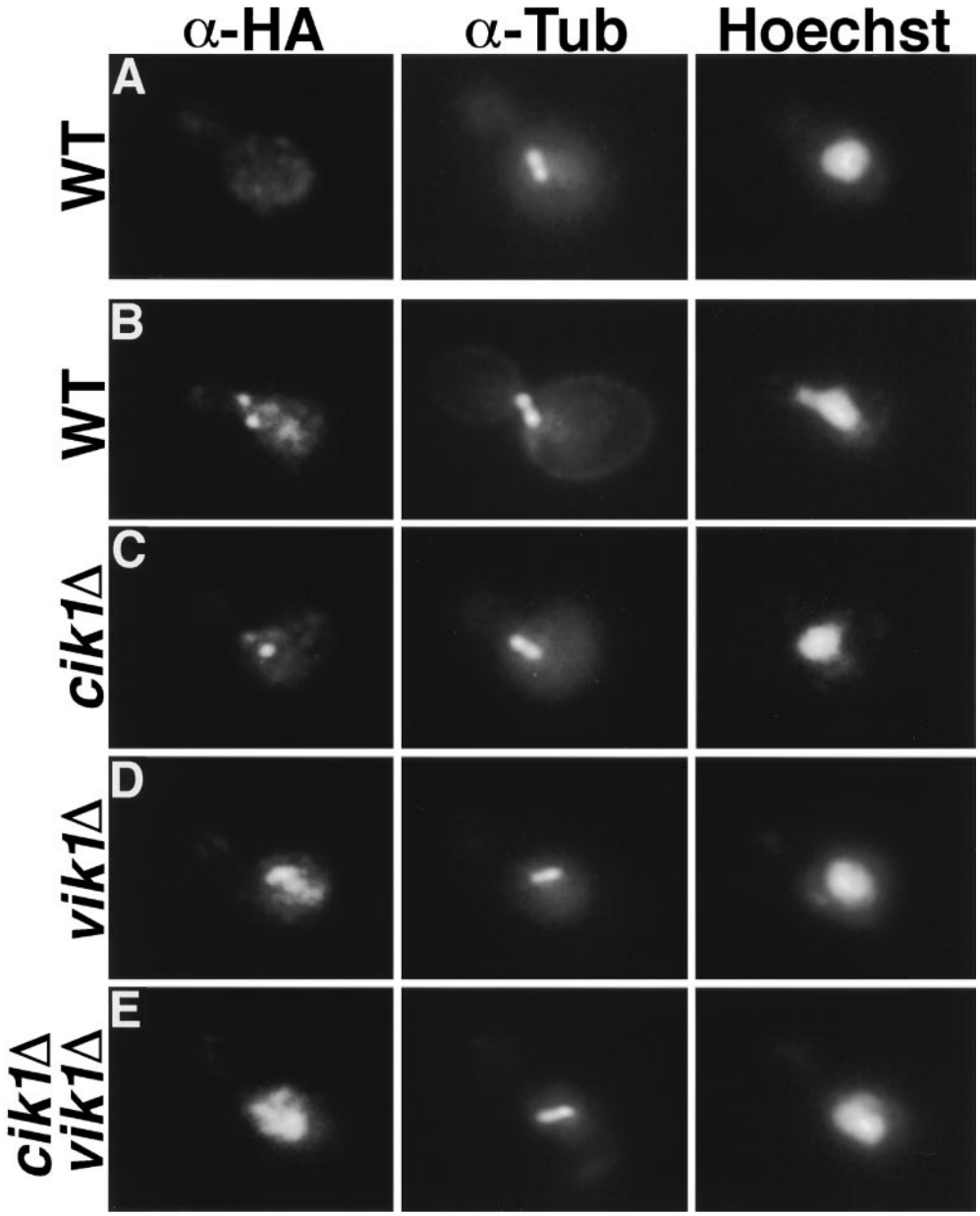

Figure 6. Concentrated localization of Kar3p to the spindle-pole bodies depends on Vik1p. Cells from growing cultures of *KAR3* untagged strain Y1869 (A) and *Kar3::HAT* haploid segregants from strain Y1753 (B–E) were prepared for indirect immunofluorescence microscopy with anti-HA antibodies (left), anti-Tub2p antibodies (middle), and Hoechst 33258 staining (right). Representative preanaphase cells are pictured: (A) an untagged cell demonstrating background staining; (B) a wild-type cell with Kar3p-HAT staining primarily at the spindle poles, as well as faint patches confined to the nucleus (as determined by overlapping Hoechst staining); (C) a *cik1Δ* cell with Kar3p-HAT remaining at the spindle-poles, the nuclear patch staining is diminished in these cells; (D) a *vik1Δ* cell with Kar3p-HAT mislocalized to spindle microtubules and bright nuclear patches, and; (E) a *cik1Δ vik1Δ* cell with Kar3p-HAT mislocalized to bright patches more diffusely distributed throughout the nucleus.

sitive growth, enhanced cytoplasmic microtubules, and the ability to properly localize Vik1p-3Xmyc to the SPBs (Meluh and Rose, 1990; Page et al., 1994; Bascom-Slack and Dawson, 1997; Saunders et al., 1997a). Fully complementing alleles were sequenced and found to lie within the region encoding the NH_2-terminal globular domain of Kar3p (data not shown). A strain containing one of these *KAR3::HAT* alleles (encoding Kar3p with the 93–amino acid HAT insertion at S^{68}) was used for immunofluorescence analysis with anti-HA antibodies.

Localization of Kar3p-HAT was examined in wild-type, *cik1Δ*, *vik1Δ*, and *cik1Δ vik1Δ* strains. Asynchronous cultures of haploid segregants from a *cik1Δ/CIK1 vik1Δ/VIK1 KAR3::HAT/KAR3::HAT* diploid strain were fixed and prepared for immunofluorescence with anti-HA and anti-tubulin antibodies (see Materials and Methods). *KAR3::HAT* wild-type cells, in all stages of the cell cycle, display anti-HA staining concentrated at the SPB region, as well as faint patches confined to the nucleus (as determined by colocalization with anti-tubulin and Hoechst staining, respectively). These fluorescence patterns are not observed in *KAR3* untagged strains, in which background staining is restricted to the cytoplasm (Fig. 6 A). Consistent with previous Kar3p localization studies (Page et al., 1994; Saunders et al., 1997), Kar3p-HAT staining is brightest at the poles of preanaphase spindles (Fig. 6 B; Table II). Most cells in G1 (80%, 100 G1 cells counted) and anaphase (86%, 100 anaphase cells counted) also display Kar3p-HAT localization at the SPBs, but this staining is fainter than that observed in preanaphase cells (data not shown). In contrast to previous studies, Kar3p-HAT localization along spindle microtubules is not detected in any stage of the cell cycle. When cytoplasmic microtubules are observed, in wild-type cells or the mutant cells described be-

Table II. Quantitation of Kar3p Localization in Preanaphase Cells

Strain	% Kar3p-HAT localization 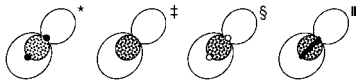				N
WT	100	0	0	0	200
cik1Δ	100¶	0	0	0	200
vik1Δ	0	44	22	34	172
cik1Δ vik1Δ	0	84	9	7	174

Anti-HA staining of asynchronous cells from isogenic Y1753 haploid segregants was used to quantitate Kar3p-HAT localization in preanaphase cells by immunofluorescence. Four different localization patterns were observed:
*Bright SPB staining with faint nuclear patches.
‡Bright nuclear patch staining.
§Bright nuclear patches and faint SPB staining.
‖Bright nuclear patches and spindle-microtubule staining.
¶Nuclear patch staining was diminished in *cik1Δ* cells.

low, Kar3p-HAT localization is not detected along their lengths. Hence, Kar3p is most abundant at the SPBs of cells throughout the cell cycle.

The effect of disrupting Vik1p and Cik1p function on Kar3p-HAT localization was determined. Since wild-type localization is most obvious in preanaphase cells, we quantified Kar3p-HAT staining patterns in cells from asynchronous cultures at this stage (Table II). Similar to wild-type strains, *KAR3::HAT cik1Δ* cells display anti-HA staining at the SPBs during all stages of the cell cycle; again, the brightest staining is observed at the poles of the preanaphase spindle (Fig. 6 C; Table II). However, the nuclear patch staining detected in wild-type cells is qualitatively diminished in the *cik1Δ* mutant. Therefore, as described previously (Page et al., 1994), Cik1p is not required to localize Kar3p to the SPBs during the vegetative cell cycle.

In contrast, Kar3p-HAT localization during vegetative growth is dramatically altered in *vik1Δ* cells (Fig 6 D; Table II). Kar3p-HAT is no longer concentrated at the SPBs in these cells; instead, it predominantly displays a bright nuclear patch localization in all *vik1Δ* cells. Moreover, staining along the lengths of spindle microtubules is detected in many cells (34% of preanaphase cells; Fig 6 D; Table II). Some *vik1Δ* cells also display faint staining in the vicinity of the SPBs, but not along spindle microtubules (22% of preanaphase cells; Table II). Therefore, although *vik1Δ* cells may retain some Kar3p at the SPBs, Vik1p is required to concentrate, or restrict, Kar3p localization to the SPBs.

To determine if the spindle and faint SPB localization of Kar3p detected in *vik1Δ* cells is due to Cik1p function, we localized Kar3p-HAT in a *cik1Δ vik1Δ* double mutant. Kar3p-HAT localization is even more aberrant in the double mutant, with the nuclear patch staining distributed more diffusely throughout the nucleus in all cells (representative preanaphase cell shown in Fig. 6 E). Detection of Kar3p-HAT along the spindle or at the SPBs in these cells is greatly reduced compared with the *vik1Δ* mutant (spindle and faint SPB localization is observed in 7 and 9%, respectively, of *cik1Δ vik1Δ* preanaphase cells; Table II). Introduction of a CEN plasmid encoding *VIK1* into either *vik1Δ* or *cik1Δ vik1Δ* mutants completely restores Kar3p-HAT concentration at the SPBs (data not shown). Therefore, during vegetative growth, Vik1p is primarily responsible for SPB targeting, or retention, of Kar3p. Cik1p may mediate Kar3p localization to less concentrated sites within the nucleus, such as the spindle and/or nuclear patches.

CIK1 and VIK1 Disruptions Result in Distinct Phenotypes

Cik1p and Vik1p exhibit differences in their expression patterns, and deletion of *CIK1* or *VIK1* results in unique effects on Kar3p localization. Therefore, the phenotypes resulting from disruption of *VIK1* and *CIK1* were compared. Suprisingly, *vik1Δ* mutants grow similar to wild-type strains at all temperatures. Using a sectoring assay described previously (Spencer et al., 1990), we determined that, unlike *cik1Δ* mutants that have a severe chromosome loss defect (Page and Snyder, 1992), *vik1Δ* mutants display only a threefold increase in frequency of chromosome loss per cell division relative to wild-type strains (data not shown). Furthermore, consistent with its absence in mating-pheromone treated cells, *vik1Δ* mutants are not defective in karyogamy, as determined by qualitative mating assays. However, compared with wild-type strains, *vik1Δ* mutants are resistant to the microtubule-depolymerizing drug benomyl (on plates containing 10, 20, or 30 μg/ml benomyl; 10 μg/ml in Fig. 7 C). The benomyl resistance phenotype always segregates with the *vik1Δ* mutation (11 tetrads analyzed).

To analyze whether *CIK1* and *VIK1* are functionally redundant, we tested whether expression of *VIK1* from a high copy plasmid could suppress the temperature-sensitive growth defect of a *cik1Δ* mutant. *cik1Δ* strains containing either the *VIK1* plasmid or vector alone are equally affected by growth at the restrictive temperature (data not shown). A *cik1Δ* mutant was then mated with a *vik1Δ* mutant, and the resulting heterozygous diploid strain was sporulated. Haploid segregants from tetratype tetrads were then analyzed (eight tetrads analyzed; results from a representative tetrad are shown in Fig. 7). Wild-type, *cik1Δ*, *vik1Δ*, and *cik1Δ vik1Δ* segregants all display similar growth on rich medium at 23°C (Fig. 7 A). However, *cik1Δ* mutants are temperature sensitive for growth at 37°C (Page and Snyder, 1992), whereas *vik1Δ* mutants grow like wild-type strains (Fig. 7 B). Suprisingly, *cik1Δ vik1Δ* double mutants grow substantially better at 37°C than *cik1Δ* mutants (Fig. 7 B). This result indicates that disruption of *VIK1* partially suppresses the temperature-sensitive growth defect of *cik1Δ* mutants. The temperature-sensitive growth defect can be restored to a *cik1Δ vik1Δ* double mutant by introduction of a CEN plasmid encoding *VIK1* (data not shown). Deletion of *VIK1* also partially suppresses the mitotic delay of *cik1Δ* mutants, as scored by the percentage of large budded cells with a single preanaphase nucleus in logarithmic phase cultures growing at 30°C (Fig. 7 D). 54% of cells from *cik1Δ* cultures exhibit the mitotic delay phenotype, whereas only 36% of cells from *cik1Δ vik1Δ* cultures have this phenotype. Wild-type and *vik1Δ* cultures each have 22% large budded cells. These strains were also analyzed for growth

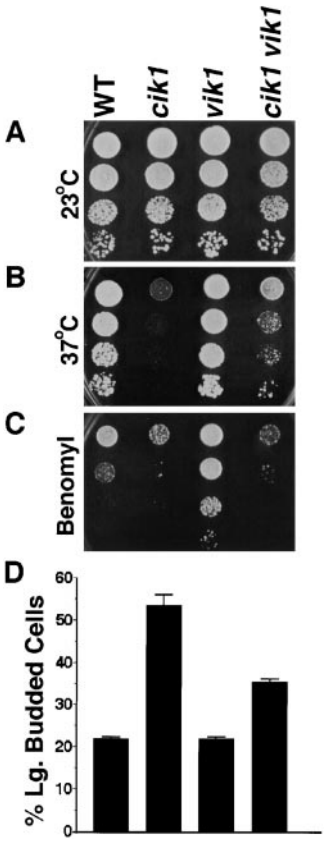

Figure 7. Phenotypic analysis of isogenic wild-type, *cik1Δ*, *vik1Δ*, and *cik1Δ vik1Δ* strains. Isogenic haploid segregants from a tetratype tetrad of the *cik1Δ/CIK1 vik1Δ/VIK1* double heterozygous diploid strain Y1738 were grown overnight to stationary phase. 10-fold serial dilutions with a starting concentration of 1×10^6 cells/ml were spotted in 5 μl drops onto agar plates containing either rich medium (A and B) or rich medium with 10 μg/ml benomyl (C). Plates were incubated for four days at either 23°C (A and C) or 37°C (B). (A) Growth on rich medium at 23°C was similar for all four strains. (B) Wild-type and *vik1Δ* growth is indistinguishable at 37°C, whereas *cik1Δ* growth is temperature sensitive. The *cik1Δ vik1Δ* double mutant grows better at the elevated temperature than *cik1Δ* mutants. (C) Compared with growth of the wild-type strain on benomyl, the *vik1Δ* mutant is more benomyl resistant, and the *cik1Δ* and *cik1Δ vik1Δ* mutants are more benomyl sensitive. (D) Cells from mid-logarithmically growing cultures of wild-type, *cik1Δ*, *vik1Δ*, and *cik1Δ vik1Δ* haploid segregants of Y1738 were stained with Hoechst 33258 and large budded cells with a single preanaphase nucleus were counted. The percentage of these cells present in the total population counted is shown. The results represent the average of two experiments in each of which greater than 300 total cells were counted for each strain.

differences in the presence of benomyl (Fig. 7 C). Unlike *vik1Δ* mutants, which display increased resistance to benomyl, *cik1Δ* and *cik1Δ vik1Δ* mutants are slightly more sensitive than wild-type strains. Therefore, the phenotypic differences of *cik1Δ* and *vik1Δ* mutants, combined with their different effects on Kar3p localization, suggest that Cik1p and Vik1p are functionally distinct.

The microtubules of the different mutant strains were examined in fixed cells from asynchronous or hydroxyurea-arrested cultures by immunofluorescence with antitubulin antibodies. Under these conditions, the microtubules of *vik1Δ* mutants are indistinguishable from those of wild-type strains. As described previously, *cik1Δ* mutants have very short spindles compared with wild-type strains and have longer, more abundant cytoplasmic microtubules (Page and Snyder, 1992). This phenotype is identical to that reported for *kar3Δ* mutants (Meluh and Rose, 1990; Saunders et al., 1997). *cik1Δ vik1Δ* double mutants display microtubules with no significant difference in length or number to those of *cik1Δ* mutants (data not shown). Therefore, if disruption of *VIK1* results in defects in microtubule structure, these defects are not detected under these conditions. Finally, consistent with the hypothesis that Cik1p and Vik1p function in complexes with Kar3p, the growth rate and microtubule phenotypes of *kar3Δ*, *kar3Δ cik1Δ*, *kar3Δ vik1Δ*, and *kar3Δ cik1Δ vik1Δ* mutants are all very similar (data not shown).

Loss of Vik1p Function Suppresses the cin8-3 kip1Δ Mutant

One vegetative function of Kar3p may be to oppose the action of two other *S. cerevisiae* KRPs, the redundant Cin8p and Kip1p motors (Hoyt et al., 1992, 1993; Saunders and Hoyt, 1992; Saunders et al., 1997b). This Kar3p function has been proposed primarily due to genetic interactions between mutations in the genes encoding these KRPs. Disruption of Cin8p and Kip1p function, using the conditional *cin8-3 kip1Δ* mutant, results in a temperature-sensitive growth defect at 35°C that is partially suppressed by disruption of Kar3p function (Saunders and Hoyt, 1992; Hoyt et al., 1993; see below). However, disruption of *CIK1*, encoding a Kar3p KAP, does not suppress *cin8-3 kip1Δ* (Fig. 8; Page et al., 1994), suggesting that the Kar3p activity that opposes Cin8p and Kip1p is independent of Cik1p.

Since Vik1p was identified as a second KAP for Kar3p during vegetative growth, we tested whether disruption of Vik1p function could suppress the temperature-sensitive growth defect of the *cin8-3 kip1Δ* mutant. *VIK1*, *CIK1*, and *KAR3* were deleted individually from the *cin8-3 kip1Δ* strain, and the resulting mutants were examined for growth defects at 23 and 35°C (Fig. 8). As demonstrated previously, the *cin8-3 kip1Δ kar3Δ* mutant grows significantly better than the original *cin8-3 kip1Δ* mutant at the restrictive temperature of 35°C (Saunders and Hoyt, 1992; Hoyt et al., 1993). Likewise, disruption of *VIK1* also partially suppresses the *cin8-3 kip1Δ* temperature-sensitive growth defect, as the *cin8-3 kip1Δ vik1Δ* mutant grows at 35°C. Introduction of a CEN plasmid encoding *VIK1* into the *cin8-3 kip1Δ vik1Δ* mutant restores temperature sensitivity to levels identical to the *cin8-3 kip1Δ* mutant (data not shown). In contrast, growth of the *cin8-3 kip1Δ cik1Δ*

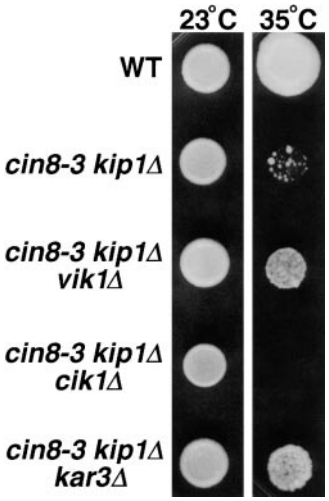

Figure 8. The temperature-sensitive growth defect of the *cin8-3 kip1Δ* mutant is suppressed by disruption of *KAR3* or *VIK1*, but not *CIK1*. Overnight cultures were grown to stationary phase, diluted down to 5×10^6 cells/ml, and 5-μl spots were plated to rich medium then incubated for three days at 23 or 35°C. Pictured are wild-type strain Y1731 and *cin8-3 kip1Δ* mutant strains Y818, *vik1Δ* Y1748, *cik1Δ* Y1758, and *kar3Δ* Y1759.

mutant is significantly diminished at all temperatures compared with the *cin8-3 kip1Δ* mutant, suggesting a possible added defect in the triple mutant. Therefore, like Kar3p, Vik1p functions antagonistically to Cin8p and Kip1p. This result further indicates that Cik1p and Vik1p are involved in distinct Kar3p functions.

Discussion

Cik1p is a previously described kinesin-associated protein that interacts with the yeast KRP Kar3p (Page and Snyder, 1992; Page et al., 1994). We have characterized a Cik1p-homologous protein called Vik1p that is present in vegetatively growing cells but, unlike Cik1p, is not detected in mating-pheromone treated cells. Coimmunoprecipitation experiments demonstrate that Vik1p also physically associates with Kar3p and that the Kar3p-Vik1p complex is separate from that of Kar3p and Cik1p. Therefore, Kar3p interacts with two different KAPs to form distinct complexes within the same cell.

Kar3p and Vik1p Are Interdependent for Proper Localization to the SPBs of Vegetatively Growing Cells

Vik1p requires Kar3p function for its SPB localization. This suggests that Kar3p-Vik1p complex formation and, presumably, the minus-end directed microtubule-motor activity of Kar3p are required to deliver Vik1p to the SPB. In the absence of Kar3p, Vik1p mislocalizes to cytoplasmic patches and is excluded from the nucleus. In contrast, Cik1p mislocalizes throughout the nucleus in the absence of Kar3p during vegetative growth (Page et al., 1994). Two possible models for Vik1p localization can be invoked. First, Vik1p may require association with Kar3p for its nuclear import. In support of this idea, Vik1p does not have sequences predicting a nuclear localization signal. Moreover, Kar3p can target to the nucleus independent of both Cik1p and Vik1p (Page et al., 1994; this study). This nuclear import of Vik1p by association with Kar3p would be analogous to the nuclear import of the yeast γ-tubulin complex. The import of this complex, and its subsequent binding to the nuclear face of the SPB, requires the nuclear localization signal of one of its components, Spc98p (Pereira et al., 1998). Alternatively, the Kar3p-Vik1p complex may be associated primarily with the cytoplasmic face of the SPB. Therefore, absence of Kar3p would result in release of Vik1p to the cytoplasm specifically, as observed. At this point, we cannot distinguish between these two possibilities, but future studies will address whether the Kar3p-Vik1p complex is on the nuclear, cytoplasmic, or both faces of the SPB.

We demonstrate that, whereas Cik1p is required to localize Kar3p to the SPBs and cytoplasmic microtubules of mating pheromone-treated cells (Page et al., 1994), Vik1p is required for proper concentration of Kar3p at the SPBs of vegetatively growing cells. In the absence of Vik1p, Kar3p mislocalizes to nuclear patches, and can be seen along spindle microtubules in many cells. Therefore, Vik1p is required for proper targeting and/or maintenance of Kar3p at the SPB. Vik1p might mediate interactions between Kar3p and other proteins that tether the complex to the SPB. Alternatively, Vik1p could prevent release of Kar3p from the minus-ends of microtubules, where its motor activity would cause it to accumulate.

In the absence of both Cik1p and Vik1p, Kar3p again mislocalizes but is more diffuse throughout the nucleus. This suggests that Cik1p may be partially redundant with Vik1p for targeting Kar3p to the SPB. However, Cik1p's primary vegetative function may be to direct localization of Kar3p to other sites within the nucleus, such as nuclear patches and the spindle. This is supported by the observation that the faint nuclear patch staining of Kar3p seen in wild-type cells is diminished in *cik1Δ* cells. Detection of Kar3p at these sites is greatly enhanced in the absence of its Vik1p-mediated SPB localization.

Finally, since some residual SPB staining can be detected in a small percentage of *cik1Δ vik1Δ* cells, Kar3p may have an inherent KAP-independent ability to localize to the SPB. This localization is likely to depend on its minus-end directed microtubule motor domain, rather than its non-motor stalk and tail domains. These latter regions of Kar3p have been shown previously to be sufficient for its spindle and SPB localization (Meluh and Rose, 1990; Page et al., 1994). Cik1p and Vik1p presumably target Kar3p to various sites of action through interactions with its nonmotor domain.

Kar3p Forms Three Functionally Distinct Complexes during the Yeast Life Cycle

Phenotypic, genetic, and biochemical analysis of Kar3p, by several different groups (Meluh and Rose, 1990; Roof et al., 1991; Saunders and Hoyt, 1992; Hoyt et al., 1993; Endow et al., 1994; Middleton and Carbon, 1994; Cottingham and Hoyt, 1997; DeZwaan et al., 1997; Saunders et al., 1997a; Huyett et al., 1998), has strongly suggested that Kar3p is a multifunctional KRP. An intriguing question in the study of molecular motors is how can one motor protein perform several different functions within a single cell. Our results indicate that Kar3p interacts with two related proteins to form three complexes that are involved in distinct microtubule-mediated cellular processes. We believe that the ability of Kar3p to interact with these associated proteins is crucial to its functional versatility. The exact molecular functions of each of these Kar3p complexes are yet to be defined. However, based on phenotypic and genetic analysis, as well as localization studies, our data reveal some possible general roles for the Kar3p-Cik1p complex during mating and the Kar3p-Cik1p and Kar3p-Vik1p complexes during mitosis (Fig. 9).

The best defined of Kar3p's functions is its role in the nuclear congression step of karyogamy, during which it associates with Cik1p (Meluh and Rose, 1990; Page et al., 1994). This complex localizes to cytoplasmic microtubules even in the absence of the Kar3p motor domain (Meluh and Rose, 1990; Page and Snyder, 1992; Page et al., 1994), indicating that the nonmotor region of the complex also has microtubule-binding capacity. In the absence of either of these two proteins, microtubules from the SPBs of opposing mating partners fail to interdigitate (Meluh and Rose, 1990; Page et al., 1994). Together, these results suggest a model in which the Kar3p-Cik1p complex acts as a cross-linker between antiparallel microtubules emanating from the SPBs of mating partners. The minus-end directed

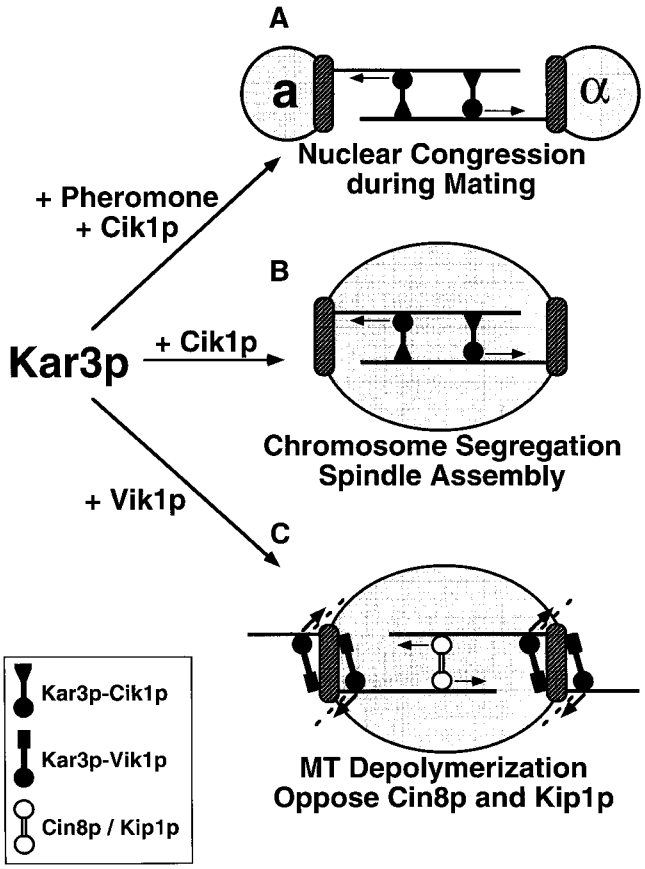

Figure 9. Schematic representation of possible functions for Kar3p complexes during the yeast life cycle. Motors and motor complexes are shown as described in the figure legend. The kinesin-related motor domains of these proteins are represented by circles, and the directionality of the motor is indicated by an arrow. The area within the nucleus is indicated by gray shading, whereas SPBs and associated microtubules are represented by the striped regions on the periphery of the nucleus and the heavy lines emanating from these region, respectively. (A) During mating, Kar3p associates with Cik1p which holds the motor in the cytoplasm in response to pheromone. After cell fusion, the Kar3p-Cik1p complex is responsible for the nuclear congression step of karyogamy. This is accomplished by cross-linking and sliding antiparallel microtubules from opposing SPBs past one another, thereby pulling the *MATa* and *MATα* nuclei together. (B) Kar3p interacts with Cik1p during vegetative growth as well. The Kar3p-Cik1p complex is in the nucleus during mitosis, where it may again act as a cross-linking/sliding motor. In this model, Kar3p-Cik1p would exert an inwardly directed force on the mitotic spindle. This force may create a tension required for proper spindle assembly and chromosome segregation since both *cik1* and *kar3* mutants have strong defects in these processes. (C) Kar3p also interacts with Vik1p during vegetative growth. The Kar3p-Vik1p complex functions primarily at the SPBs, either on the cytoplasmic face, the nuclear face, or both. Based on phenotypic and genetic analysis, this complex may have microtubule-depolymerizing activity that opposes the SPB separating force generated by Cin8p and Kip1p.

microtubule-motor activity of Kar3p can then create the force that pulls the nuclei together by sliding cross-linked microtubules past one another (Fig. 9 A).

Despite many studies on the function of Kar3p during vegetative growth, its role during mitosis remains obscure. Our identification of two Kar3p-interacting proteins with distinct Kar3p-related vegetative phenotypes should help elucidate the exact mitotic functions of this KRP. Disruption of either *KAR3* or *CIK1* results in similar mitotic phenotypes, including very short spindles indicative of a spindle assembly defect (Meluh and Rose, 1990; Page and Snyder, 1992; Saunders et al., 1997a) and a mitotic delay mediated by the spindle-assembly checkpoint (Roof et al., 1991; Manning, B.D., J.A. Wallace, and M. Snyder, unpublished observation). Unlike during mating, the Kar3p-Cik1p complex is in the nucleus during the mitotic cell cycle, where it associates with the SPBs and, to a lesser extent, spindle microtubules (Page and Snyder, 1992; Page et al., 1994; Saunders et al., 1997a). Analogous to its role in karyogamy, the complex may act within the spindle to cross-link and slide antiparallel microtubules from opposing SPBs past one another, thereby creating an inward force on the spindle (Fig. 9 B). This force may generate a tension important for proper spindle assembly. Alternatively, the Kar3p-Cik1p microtubule cross-linking activity could be crucial to the organization of a bipolar spindle. This spindle assembly defect would account for the chromosome instability phenotype of *cik1Δ* mutants (Page and Snyder, 1992). Additionally, it is possible that this complex could play a more direct role in chromosome segregation, perhaps as a kinetochore motor (Hyman et al., 1992; Middleton and Carbon, 1994).

Kar3p is likely to have a separate mitotic function that is mediated by interaction with Vik1p at the SPBs. The benomyl resistance phenotype of *vik1Δ* mutants, suggests that the Kar3p-Vik1p complex may be involved in microtubule depolymerization (Fig. 9 C). The motor domain of Kar3p has been shown to possess minus-end–specific microtubule-depolymerizing activity in vitro (Endow et al., 1994), and has been suggested by phenotypic analysis to depolymerize microtubules in vivo (Saunders et al., 1997). Kar3p complexed with Vik1p, specifically, might possess this activity. Alternatively, Kar3p may require interaction with Vik1p to prevent release from microtubule minus ends where it catalyzes microtubule depolymerization. At this point, it is unclear whether this complex acts on cytoplasmic microtubules, the spindle, or both. Disruption of *VIK1* does not result in any detectable differences in the microtubule structures of fixed cells compared with wild-type strains. It is possible that accumulation of Kar3p on the spindle, observed in *vik1Δ* mutants, could stabilize these microtubules and account for the benomyl resistance phenotype.

Based on genetic analysis, Kar3p-Vik1p function is detrimental to mutants lacking the plus-end–directed Cin8p and Kip1p KRPs. These proteins are members of the BimC family of KRPs and are believed to act as homotetrameric bipolar motor proteins that generate a SPB separating force during spindle assembly and anaphase B (Hoyt et al., 1992; Saunders et al., 1995; Kashina et al., 1997; Straight et al., 1998). Disruption of either *KAR3* or *VIK1* can suppress the temperature-sensitive growth defect of the *cin8-3 kip1Δ* mutant, suggesting that the Kar3p-Vik1p complex may oppose the function of Cin8p and Kip1p (Fig. 9 C; Saunders and Hoyt, 1992; Hoyt et al., 1993). Interestingly, a *TUB2* mutation that stablilizes mi-

crotubules can also suppress this mutant (Saunders et al., 1997a), suggesting that a defect in the putative microtubule depolymerizing activity of the Kar3p-Vik1p complex could be sufficient for suppression of *cin8-3 kip1Δ*.

The functional interactions between the two vegetative Kar3p complexes may be complicated. For example, disruption of *VIK1* partially suppresses the temperature-sensitive growth defect and mitotic delay of *cik1Δ* mutants. One interpretation of this result is that the two Kar3p complexes partially oppose one another. It is also interesting to note that *cik1Δ* mutants, in which Kar3p's SPB localization is unperturbed, have much stronger phenotypes (Page and Snyder, 1992) than those of *vik1Δ* mutants, in which Kar3p is no longer concentrated at the SPBs. Therefore, the most critical of Kar3p functions during vegetative growth may occur at sites other than the spindle poles. Future studies will address these issues, but it is clear from our current study that Cik1p and Vik1p are not functionally redundant.

KRP Regulation and Targeting by Kinesin-associated Proteins

In general, the functional specificity of KRPs is determined by their nonmotor domains. Some KRPs can target to their sites of action independent of associated proteins. For example, the *Drosophila* Nod protein, involved in chromosome movements during mitosis, contains a DNA binding motif in its nonmotor domain (Afshar et al., 1995). However, the targeting of many KRPs will likely be mediated through complex formation with nonmotor subunits (i.e., KAPs). The highly divergent nature of the nonmotor domains of KRPs (reviewed by Goldstein, 1993; Vale and Fletterick, 1997) suggest that interacting proteins will also be diverse in sequence. Nevertheless, we expect that mechanisms of motor targeting by KAPs will exist that are universal.

The light chains of conventional kinesin are the most studied of all KAPs. Several different KLCs can exist within a single cell (Cyr et al., 1991; Beushausen et al., 1993; Wedaman et al., 1993; Rahman et al., 1998), and these are thought to control the cargo-binding specificity of KHCs (Khodjakov et al., 1998; Liao and Gundersen, 1998). Therefore, it is possible that different KLCs target kinesin to distinct membranous organelles and vesicles, and it has been suggested that KLC mediates the interaction between kinesin and membranes (Stenoien and Brady, 1997). Additionally, KLCs might regulate KHC-microtubule binding and/or motor activity by contacting the motor domain when kinesin is in a folded confirmation (Hackney et al., 1992; Verhey et al., 1998).

Little is known about the regulation and targeting of specific KRPs. The tail domain of the *Xenopus* mitotic KRP, Xklp2, has recently been shown to require cytoplasmic dynein and a microtubule-associated protein, TPX2, to localize to spindle poles (Wittmann et al., 1998). However, these proteins are not tightly associated KAPs. Our results demonstrate that Kar3p localization is regulated through its interaction with two different KAPs, Cik1p and Vik1p (Page et al., 1994; this study). These KAPs control various Kar3p functions, at least in part, by targeting the motor to discrete sites within the cell. Whether Cik1p and Vik1p modulate motor activity once Kar3p is at these sites is not yet known. The study of these proteins should define regulatory strategies used by other KRPs and help elucidate general elements underlying the functional diversity of KRPs.

We thank C. Horak and J. Vogel for critical comments on the manuscript. We are grateful to L.L. Satterwhite, P.B. Meluh, and M.D. Rose for providing the anti-Kar3p antibodies, F. Solomon for the anti-Tub2p antibodies, and M.A. Hoyt for the *cin8-3 kip1Δ* strain.

B.D. Manning and J.G. Barrett were supported by National Institutes of Health (NIH) training grants and NIH grants GM3649 and GM52197, and this research was funded by NIH grant GM52197.

Received for publication 24 December 1998 and in revised form 18 February 1999.

References

Afshar, K., J. Scholey, and R.S. Hawley. 1995. Identification of the chromosome localization domain of the *Drosophila* Nod kinesin-like protein. *J. Cell Biol.* 131:833–843.

Arnal, I., F. Metoz, S. DeBonis, and R.H. Wade. 1996. Three-dimensional structure of functional motor proteins on microtubules. *Curr. Biol.* 6:1265–1270.

Bascom-Slack, C.A., and D.S. Dawson. 1997. The yeast motor protein, Kar3p, is essential for meiosis I. *J. Cell Biol.* 139:459–467.

Beushausen, S., A. Kladakis, and H. Jaffe. 1993. Kinesin light chains: identification and characterization of a family of proteins from the optic lobe of the squid *Loligo pealii*. *DNA Cell Biol.* 12:901–909.

Bond, J., J. Fridovich-Keil, L. Pillus, R. Mulligan, and F. Solomon. 1986. A chicken-yeast chimeric beta-tubulin protein is incorporated into mouse microtubules *in vivo*. *Cell.* 44:461–468.

Burns, N., B. Grimwade, P.B. Ross-Macdonald, E.-Y. Choi, K. Finberg, G.S. Roeder, and M. Snyder. 1994. Large-scale characterization of gene expression, protein localization and gene disruption in *Saccharomyces cerevisiae*. *Genes Dev.* 8:1087–1105.

Cole, D.G., S.W. Chinn, K.P. Wedaman, K. Hall, T. Vuong, and J.M. Scholey. 1993. Novel heterotrimeric kinesin-related protein purified form sea urchin eggs. *Nature.* 366:268–270.

Cole, D.G., D.R. Diener, A.L. Himelblau, P.L. Beech, J.C. Fuster, and J.L. Rosenbaum. 1998. *Chlamydomonas* kinesin-II–dependent intraflagellar transport (IFT): IFT particles contain proteins required for ciliary assembly in *Caenorhabditis elegans* sensory neurons. *J. Cell Biol.* 141:993–1008.

Cottingham, F.R., and M.A. Hoyt. 1997. Mitotic spindle positioning in *Saccharomyces cerevisiae* is accomplished by antagonistically acting microtubule motor proteins. *J. Cell Biol.* 138:1041–1053.

Cyr, J.L., K.K. Pfister, G.S. Bloom, C.A. Slaughter, and S.T. Brady. 1991. Molecular genetics of kinesin light chains: generation of isoforms by alternative splicing. *Proc. Natl. Acad. Sci. USA.* 88:10114–10118.

DeZwaan, T.M., E. Ellingson, D. Pellman, and D.M. Roof. 1997. Kinesin-related *KIP3* of *Saccharomyces cerevisiae* is required for a distinct step in nuclear migration. *J. Cell Biol.* 138:1023–1040.

Elledge, S.J., and R.W. Davis. 1988. A family of versatile centromeric vectors designed for use in the sectoring-shuffle mutagenesis assay in *Saccharomyces cerevisiae*. *Gene.* 70:303–312.

Endow, S.A., S.J. Kang, L.L. Satterwhite, M.D. Rose, V.P. Skeen, and E.D. Salmon. 1994. Yeast Kar3 is a minus-end microtubule motor protein that destabilizes microtubules preferentially at the minus ends. *EMBO (Eur. Mol. Biol. Organ.) J.* 13:2708–2713.

Gauger, A.K., and L.S.B. Goldstein. 1993. The *Drosophila* kinesin light chain. *J. Biol. Chem.* 268:13657–13666.

Gehrung, S., and M. Snyder. 1990. The *SPA2* gene of *Saccharomyces cerevisiae* is important for pheromone-induced morphogenesis and efficient mating. *J. Cell Biol.* 111:1451–1464.

Goldstein, L.S.B. 1993. With apologies to Scheherazade: tails of 1001 kinesin motors. *Annu. Rev. Genet.* 27:319–351.

Gulick, A.M., H. Song, S.A. Endow, and I. Rayment. 1998. X-ray crystal structure of the yeast Kar3 motor domain complexed with Mg.ADP to 2.3 A resolution. *Biochemistry.* 37:1769–1776.

Guthrie, C., and G.R. Fink. 1991. Guide to yeast genetics and molecular biology. *Methods Enzymol.* 194:1–933.

Hackney, D.D., J.D. Levitt, and J. Suhan. 1992. Kinesin undergoes a 9 S to 6 S conformation transition. *J. Biol. Chem.* 267:8696–8701.

Hirokawa, N. 1996. Organelle transport along microtubules-the role of KIFs. *Trends Cell Biol.* 6:135–141.

Hirokawa, N. 1998. Kinesin and dynein superfamily proteins and the mechanism of organelle transport. *Science.* 279:519–526.

Hirose, K., A. Lockhart, R.A. Cross, and L.A. Amos. 1995. Nucleotide-dependent angular change in kinesin motor domain bound to tubulin. *Nature.* 376: 277–279.

Hirose, K., A. Lockhart, R.A. Cross, and L.A. Amos. 1996. Three-dimensional cryoelectron microscopy of dimeric kinesin and ncd motor domains on microtubules. *Proc. Natl. Acad. Sci. USA*. 93:9539–9544.

Hoyt, M.A., L. He, K.K. Loo, and W.S. Saunders. 1992. Two *Saccharomyces cerevisiae* kinesin-related gene products required for mitotic spindle assembly. *J. Cell Biol.* 118:109–120.

Hoyt, M.A., L. He, L. Totis, and W.S. Saunders. 1993. Loss of function of *Saccharomyces cerevisiae* kinesin-related *CIN8* and *KIP1* is suppressed by *KAR3* motor domain mutations. *Genetics.* 135:35–44.

Huyett, A., J. Kahana, P. Silver, X. Zeng, and W.S. Saunders. 1998. The Kar3p and Kip2p motors function antagonistically at the spindle poles to influence cytoplasmic microtubule numbers. *J. Cell Sci.* 111:295–301.

Hyman, A.A., K. Middleton, M. Centola, T.J. Mitchison, and J. Carbon. 1992. Microtubule-motor activity of a yeast centromere-binding protein complex. *Nature*. 359:533–536.

Ito, H., Y. Fukada, K. Murata, and A. Kimura. 1983. Transformation of intact yeast cells with alkali cations. *J. Bacteriol.* 153:163–168.

Kashina, A.S., G.C. Rogers, and J.M. Scholey. 1997. The bimC family of kinesins: essential bipolar mitotic motors driving centrosome separation. *Biochim. Biophys. Acta.* 1357:257–271.

Khodjakov, A., E.M. Lizunova, A.A. Minin, M.P. Koonce, and F.K. Gyoeva. 1998. A specific light chain of kinesin associates with mitochondria in cultured cells. *Mol. Biol. Cell.* 9:333–343.

Kronstad, J.W., J.A. Holly, and V.L. MacKay. 1987. A yeast operator overlaps an upstream activation site. *Cell.* 50:369–377.

Kull, F.J., E.P. Sablin, R. Lau, R.J. Fletterick, and R.D. Vale. 1996. Crystal structure of the kinesin motor domain reveals a structural similarity to myosin. *Nature*. 380:550–555.

Kurihara, L.J., B.G. Stewart, A.E. Gammie, and M.D. Rose. 1996. Kar4p, a karyogamy-specific component of the yeast pheromone response pathway. *Mol. Cell. Biol.* 16:3990–4002.

Laemmli, U.K. 1970. Cleavage of structural proteins during the assembly of the head of bacteriophage T4. *Nature*. 227:680–685.

Liao, G., and G.G. Gundersen. 1998. Kinesin is a candidate for cross-bridging microtubules and intermediate filaments. *J. Biol. Chem*. 273:9797–9803.

Lindesmith, L., J.M. McIlvain, Y. Argon, and M.P. Sheetz. 1997. Phosphotransferases associated with the regulation of kinesin motor activity. *J. Biol. Chem*. 272:22929–22933.

Lupas, A. 1996. Prediction and analysis of coiled-coil structures. *Methods Enzymol.* 266:513–525.

Lupas, A., M.V. Dyke, and J. Stock. 1991. Predicting coiled coils from protein sequences. *Science.* 252:1162–1164.

Manning, B.D., R. Padmanabha, and M. Snyder. 1997. The Rho-GEF Rom2p localizes to sites of polarized cell growth and participates in cytoskeletal functions in *Saccharomyces cerevisiae. Mol. Biol. Cell*. 8:1829–1844.

McIlvain, J.M., J.K. Burkhardt, S. Hamm-Alvarez, Y. Argon, and M.P. Sheetz. 1994. Regulation of kinesin activity by phosphorylation of kinesin-associated proteins. *J. Biol. Chem*. 269:19176–19182.

Meluh, P.B., and M.D. Rose. 1990. *KAR3*, a kinesin-related gene required for yeast nuclear fusion. *Cell.* 60:1029–1941.

Middleton, K., and J. Carbon. 1994. *KAR3*-encoded kinesin is a minus-end-directed motor that functions with centromere binding proteins (CBF3) on an *in vitro* yeast kinetochore. *Proc. Natl. Acad. Sci. USA*. 91:7212–7216.

Moore, J.D., and S.A. Endow. 1996. Kinesin proteins: a phylum of motors for microtubule-based motility. *Bioessays*. 18:207–219.

Page, B., and M. Snyder. 1992. CIK1: a developmentally regulated spindle pole body-associated protein important for microtubule functions in *Saccharomyces cerevisiae*. *Genes Dev*. 6:1414–1429.

Page, B.D., L.L. Satterwhite, M.D. Rose, and M. Snyder. 1994. Localization of the KAR3 kinesin heavy chain-like protein requires the CIK1 interacting protein. *J. Cell Biol.* 124:507–519.

Pereira, G., M. Knop, and E. Schiebel. 1998. Spc98p directs the yeast g-tubulin complex into the nucleus and is subject to cell cycle-dependent phosphorylation on the nuclear side of the spindle-pole body. *Mol. Biol. Cell.* 9:775–793.

Pringle, J., A.E.M. Adams, D.G. Drubin, and B.K. Haarer. 1991. Immunofluorescence methods for yeast. *Methods Enzymol.* 194:565–601.

Rahman, A., D.S. Friedman, and L.S.B. Goldstein. 1998. Two kinesin light chain genes in mice: identification and characterization of the encoded proteins. *J. Biol. Chem*. 273:15395–15403.

Roof, D., P. Meluh, and M. Rose. 1992. Kinesin-related proteins required for assembly of the mitotic spindle. *J. Cell Biol.* 118:95–108.

Roof, D.M., P. Meluh, and M. Rose. 1991. Multiple kinesin-related proteins in yeast mitosis. *Cold Spring Harbor Symp. Quant. Biol.* 61:693–703.

Ross-MacDonald, P., A. Sheehan, G.S. Roeder, and M. Snyder. 1997. A multipurpose transposon system for analyzing protein production, localization, and function in *Saccharomyces cerevisiae*. *Proc. Natl. Acad. Sci. USA*. 94: 190–195.

Sablin, E.P., F.J. Kull, R. Cooke, R.D. Vale, and R.J. Fletterick. 1996. Crystal structure of the motor domain of the kinesin-related motor ncd. *Nature*. 380: 555–559.

Sambrook, J., E.F. Fritsch, and T. Maniatis. 1989. Molecular Cloning: A Laboratory Manual. 2nd edition. Cold Spring Harbor Laboratory Press, Cold Spring Harbor, NY.

Saunders, W., and M.A. Hoyt. 1992. Kinesin-related proteins required for structural integrity of the mitotic spindle. *Cell*. 70:451–458.

Saunders, W.S., D. Koshland, D. Eshel, I.R. Gibbons, and M.A. Hoyt. 1995. *Saccharomyces cerevisiae* kinesin- and dynein-related proteins required for anaphase chromosome segregation. *J. Cell Biol.* 128:617–624.

Saunders, W., D. Hornack, V. Lengyel, and C. Deng. 1997a. The *Saccharomyces cerevisiae* kinesin-related motor Kar3p acts at preanaphase spindle poles to limit the number and length of cytoplasmic microtubules. *J. Cell Biol.* 137: 417–431.

Saunders, W., V. Lengyel, and M.A. Hoyt. 1997b. Mitotic spindle function in *Saccharomyces cerevisiae* requires a balance between different types of kinesin-related motors. *Mol. Biol. Cell*. 8:1025–1033.

Schnapp, B.J., and T.S. Reese. 1989. Dynein is the motor for retrograde axonal transport of organelles. *Proc. Natl. Acad. Sci. USA*. 86:1548–1552.

Schneider, B.L., W. Seufert, B. Steiner, Q.H. Yang, and A.B. Futcher. 1995. Use of PCR epitope tagging for protein tagging in *Saccharomyces cerevisiae*. *Yeast.* 11:1265–1274.

Scholey, J.M. 1996. Kinesin-II, a membrane traffic motor in axons, axonems, and spindles. *J. Cell Biol.* 133:1–4.

Sikorski, R., and P. Hieter. 1989. A system of shuttle vectors and yeast host strains designed for efficient manipulation of DNA in *Saccharomyces cerevisiae*. *Genetics*. 122:19–27.

Spencer, F., S.L. Gerring, C. Connelly, and P. Hieter. 1990. Mitotic chromosome transmission fidelity mutants in *Saccharomyces cerevisiae*. *Genetics.* 124:237–249.

Stenoien, D.L., and S.T. Brady. 1997. Immunochemical analysis of kinesin light chain function. *Mol. Biol. Cell*. 8:675–689.

Steuer, E.R., L. Wordeman, T.A. Schroer, and M.P. Sheetz. 1990. Localization of cytoplasmic dynein to mitotic spindles and kinetochores. *Nature.* 345:266–268.

Straight, A.F., J.W. Sedat, and A.W. Murray. 1998. Time-lapse microscopy reveals unique roles for kinesins during anaphase in budding yeast. *J. Cell Biol.* 143:687–694.

Vale, R.D., and R.J. Fletterick. 1997. The design plan of kinesin motos. *Annu. Rev. Cell Dev. Biol.* 13:745–777.

Vale, R.D., T.S. Reese, and M.P. Sheetz. 1985. Identification of a novel force generating protein, kinesin, involved in microtubule-based motility. *Cell*. 42: 39–50.

Verhey, K.J., D.L. Lizotte, T. Abramson, L. Barenboim, B.J. Schnapp, and T.A. Rapoport. 1998. Light chain-dependent regulation of kinesin's interaction with microtubules. *J. Cell Biol.* 143:1053–1066.

Wedaman, K.P., A.E. Knight, J. Kendrick-Jones, and J.M. Scholey. 1993. Sequences of sea urchin kinesin light chain isoforms. *J. Mol. Biol.* 231:155–158.

Wedaman, K.P., D.W. Meyer, D.J. Rashid, D.G. Cole, and J.M. Scholey. 1996. Sequence and submolecular localization of the 115-kD accessory subunit of the heterotrimeric kinesin-II ($KRP_{85/95}$) complex. *J. Cell Biol.* 132:371–380.

Wittmann, T., H. Boleti, C. Antony, E. Karsenti, and I. Vernos. 1998. Localization of the kinesin-like protein Xklp2 to spindle poles requires a leucine zipper, a microtubule-associated protein, and dynein. *J. Cell Biol.* 143:673–685.

Yamazaki, H., T. Nakata, Y. Okada, and N. Hirokawa. 1996. Cloning and characterization of KAP3: a novel kinesin superfamily-associated protein of KIF3A/3B. *Proc. Natl. Acad. Sci. USA*. 93:8443–8448.

Yang, J.T., R.A. Laymon, and L.S.B. Goldstein. 1989. A three-domain structure of kinesin heavy chain revealed by DNA sequence and microtubule binding analyses. *Cell*. 56:879–889.

Yang, J.T., W. Saxton, R. Stewart, E. Raff, and L. Goldstein. 1990. Evidence that the head of kinesin is sufficient for force generation and motility in vitro. *Nature.* 249:42–47.